Spring Balancing of Prosthetic & Orthotic Devices

A Project Report

submitted by

SUSHANT VEER

in partial fulfilment of the requirements
for the award of the degree of

BACHELOR OF TECHNOLOGY

DEPARTMENT OF MECHANICAL ENGINEERING
INDIAN INSTITUTE OF TECHNOLOGY MADRAS

MAY 2013

PROJECT CERTIFICATE

This is to certify that the thesis titled **Spring Balancing of Prosthetic & Orthotic Devices**, submitted by **Sushant Veer(ME09B058)**, to the Indian Institute of Technology, Madras, for the award of the degree of **Bachelor of Technology**, is a bona fide record of the research work done by him under our supervision. The contents of this thesis, in full or in parts, have not been submitted to any other Institute or University for the award of any degree or diploma.

Prof. Sujatha Srinivasan
Guide
Associate Professor
Dept. of Mechanical Engineering
IIT-Madras, 600 036

Prof. T. Sundararajan
Head
Dept. of Mechanical Engineering
IIT-Madras, 600 036

Place: Chennai

Date: 10th May 2013

ACKNOWLEDGEMENTS

Working with Dr. Sujatha Srinivasan has been a great learning experience. I am thankful to her for giving me the opportunity to work on a project that matched my proclivity. Her incessant commitment towards the furtherance of assistive technology was a force that provided unbounded motivation for completion of this project. I am also thankful to her for giving me a chance to work on many other projects over a period of two years and for the inspired teaching that kindled my interest in the field of mechanisms.

I am grateful to Mr. Mohan Damu for occasionally helping me out with optimization and Mr. Mayank Seth for making me understand prostheses and orthoses from a clinicians point of view.

A special word of thanks for K. L. Preetish and M. Rohith for lending their ear to me and criticizing me whenever need be.

And finally I would like to thank my mother, father and sister for their constant support and motivation which urged me to keep going on no matter what the odds be.

Sushant Veer

ABSTRACT

KEYWORDS: Gravity compensation; Spring balancing; Prostheses; Orthoses; Exoskeleton; Stand-up-wheelchair.

The potential benefit of applying gravity balancing to orthotic, prosthetic and other wearable devices is well recognized, but practical applications have been difficult to achieve. Although existing methods provide exact gravity balance, they require additional masses or auxiliary links, or all the springs used originate from the ground, which makes the resulting device bulky and space-inefficient. This work presents a new method that is more practical than existing methods to provide approximate gravity balancing of mechanisms to reduce actuator loads. Current balancing methods use zero-free-length springs or simulate them to achieve balancing. Here, non-zero-free-length springs are used directly. This new method allows springs to be attached to the preceding parent link, which makes the implementation of spring balancing practical. The method is applicable to planar and spatial, open and closed kinematic chains. Applications of this method to lower-limb orthosis and prosthesis are studied in detail. Practical challenges and beginning steps towards an experimental setup are also discussed.

TABLE OF CONTENTS

LIST OF TABLES

LIST OF FIGURES

NOTATION

R_i	The position vector of the centre of mass of the ith link from the parent pivot of the ith body.
r_i	$\|R_i\|$
R_i^j	The vector R_i with respect to the coordinate system j
T_i^j	Transformation matrix from coordinate system i to j
l_i	Kinematic length of the ith linkage
β_{ij}	Angle of $\mathbf{S}_{ij}$ with respect to the kinematic line of the ith link measured counterclockwise (β_{12} is the only exception measured from horizontal)
α_i	Angle of $\mathbf{R}_i$ with respect to the kinematic line of the ith link measured counterclockwise
θ_i	Angle of the kinematic line of the ith link measured counterclockwise from horizontal (Assumed 0 for ground)
m_i	Mass of the ith link
K_i	Spring constant of the spring connecting body i and i+1
len_i	Free length of the spring connecting body i and i+1
g	acceleration due to gravity (9.8 m/s^2)
PE	Total Potential Energy
τ	Torque
F	Preload Force of gas-spring
k	K-Factor of gas-spring

CHAPTER 1

Introduction

1.1 Introduction

Gravity compensation of linkages in mechanisms to reduce actuator requirements is a well recognized concept. Gravity balancing has been used in anthropomorphic robots and other linkages which have to work against gravity. There are multiple advantages of reducing the actuator requirements.

Reduced actuator torque facilitates the use of lower end actuators which are generally smaller in weight and volume thereby lowering the space requirements and the total weight of the mechanism. This is particularly important for anthropomorphic robots where the parent actuator has to handle the weight of the subsequent actuators as well. Actuators with lower actuation requirements would be more energy efficient, thereby reducing the energy consumption of the mechanism. Lower end actuators would be lower in cost, facilitating the development of low cost devices.

The advantages of gravity compensation makes it an important tool while designing a machine. There are numerous applications of gravity compensation. It is used for ergonomic design of everyday equipment. Some such applications are gravity compensated luggage door of a car, low effort wall folding beds, table lamps that could be held static in any position and gravity balanced vertical drafters. Gravity comepnsation is also used in anthropomorphic robots and planar mechanisms that operate on a non-horizontal plane and wearable assistive devices used for therapeutic purposes or daily use. Gravity balanced assistive devices have found a very important application for gait rehabilitation of stroke patients as shown in Agrawal *et al.* (2007). Rahman *et al.* (2000) discuss the development of gravity balanced arm prosthesis. There are many other miscellaneous applications of gravity compensation like therapeutic sit-to-stand devices for people with muscular weakness as developed by Fattah *et al.* (2006).

1.2 Methods

Gravity compensation can be carried out by various methods. Some of the most common methods are - fixed position of the centre of mass of the mechanism and spring

force for counteracting the effect of gravity.

Fixed position of the centre of mass of the mechanism is normally achieved by using counter weights. The net centre of mass of the mechanism is made to reach a point which would always be stationary during the motion of the mechanism, for example the pivot between the ground link and a rotor. Spring force to counteract the effect of gravity is used as follows - when the centre of mass of the link moves down, the spring stores more energy, thus making the net potential energy, i.e., the sum of gravitational and spring potential energy to remain constant.

Using counter-weights is less preferable over using springs because even though counterweights provide gravity compensation, they increase the total mass of the mechanism and thus more energy has to be spent in moving it. Springs on the other hand provide a space efficient and comparatively lower weight solution for achieving the same result although there are some practical difficulties with springs that will be discussed ahead. In general the above two methods can be represented mathematically by any of the two ways - Constant potential energy ; Making the actuation requirement zero by solving Newtonian equations.

In this work spring balancing is studied. Generally, in the mathematical models for spring balancing, the springs are assumed of zero-free-length. A zero-free-length is a theoretical spring whose natural length is zero. Since this is not a practical scenario, zero-free-length springs have to be simulated by methods explained by Rahman *et al.* (1995); Deepak and Ananthasuresh (2009). These methods require the use of pulleys and cables increasing the weight and volume occupancy of the mechanism. Te Riele and Herder (2001) show perfect spring balancing with non-zero-free-length springs but the case covered in that work is a very specific geometrical configuration which may not be applicable to all scenarios. Thus spring balancing comes with its own set of challenges.

1.3 Literature Review

Rahman *et al.* (1995) present techniques for balancing a single link perfectly using zero-free-length springs and extend it to balancing an n-link open chain with the help of auxiliary links. Although the use of auxiliary links provides perfect balancing, the additional links occupy a lot of space and increase the mass and volume occupancy of the mechanism. In addition, these techniques assume zero-free-length springs, which further contributes to the complexity of the design because simulating zero-free-length springs require the use of pulleys and cables as discussed by Rahman *et al.* (1995);

Deepak and Ananthasuresh (2009). Similarly, Streit and Shin (1993) use zero-free-length springs for spring balancing of closed loop linkages. Agrawal and Agrawal (2005) provide an approximate static balancing method using non-zero-free length springs but with the need for auxiliary links. Te Riele and Herder (2001) present a perfect balancing technique using non-zero-free-length springs but their solution has a very specific geometric configuration and it may not be usable always due to space-size limitations. Gopalswamy *et al.* (1992) present an approximate static balancing technique for a parallelogram linkage using torsional springs. Agrawal and Fattah (2004*a*) demonstrates spring balancing of spatial linkages, but even there auxiliary linkages are used.

This work was inspired by the recent method devised by Deepak and Ananthasuresh (2012) which provides for perfect gravity balancing using only springs and no auxiliary links. However, their method again requires zero-free-length springs or the simulation thereof using non-zero-free-length springs. In addition, all the springs in their technique have one end pivoted to the ground. These conditions pose considerable problems in many situations like wearable devices where cosmetic appearance and available space are major constraints. The balancing literature seemed to lack a technique that couples the advantages of having spring balancing with non-zero-free-length springs and without the need for auxiliary links in a space efficient and generic manner to provide approximate or exact gravity compensation for reducing the actuation requirements of a mechanism.

There have been techniques for approximate spring balancing and for determining optimal spring pivot locations. Segla *et al.* (1998) presents an optimization for a six DOF robot mechanism with the gripper force as the objective function using genetic algorithm. Huang and Roth (1993, 1994) use the principle of virtual work for optimal placement of springs. Mahalingam and Sharan (1986) present an optimization for optimal location of spring pivots and relevant spring characteristics to reduce the unbalanced moment. Similarly, Brinkman and Herder (2002) present a technique for optimal spring balanced mechanisms without theoretical assumptions. Here we propose an optimization based approximate spring balancing technique that helps predict the relevant spring parameters and spring pivot locations. The technique is presented in a generic fashion which could be implemented on a variety of mechanisms.

This work is motivated by the need for practical implementation of balancing in mechanisms that have stringent space and mass constraints, like orthoses, prostheses and exoskeletons. Previous attempts at using gravity balancing for such devices have resulted in complex and bulky mechanisms (Agrawal and Fattah (2004*b*); Banala *et al.* (2006); Nakayama *et al.* (2009)). Ciupitu and Simionescu propose some mechanisms in

their work which have medical relevance but all these mechanisms have springs attached to the ceiling greatly hindering the mobility and increasing the space requirements. The attempt in this project is to develop a method for spring balancing that is generic and could be applied to varied mechanisms and overcome some of the practical difficulties faced in developing a spring balanced lower limb orthosis.

1.4 Objective & Scope

The objectives of this project are to devise a generic method for spring balancing using non-zero-free-length springs such that parent-child link connections could be made between the successive links ; Demonstration of this method for various scenarios, namely - open planar linkages, closed planar linkages, open spatial linkages, balancing with torsional springs and gas springs

Applications relating to orthoses & prostheses that were investigated include the design of springs for a lower limb orthosis using the method devised above. A comparison of hip-moment required to control a trans-femoral lower-limb prosthesis with a single axis knee, a polycentric knee and a polycentric knee coupled with spring balancing was carried out. The design of an experimental setup for spring balanced lower limb orthosis has also been accomplished.

1.5 Organization of the report

The thesis is organized as follows: Chapter 1 discusses the need for spring balancing, the literature available on it and the objectives of this work. Chapter 2 shows that perfect spring balancing is not possible by child-parent spring connections, proposes a method for approximate spring balancing and describes the problem formulation for approximate spring balancing of open-link planar chains, a four-bar linkage and open-link spatial chains. Chapter 3 demonstrates the method proposed in chapter 2 using suitable examples. Chapter 4 extends this technique to gas springs and torsional springs and also compares it with peak torque minimization. Chapter 5 covers the spring balancing of lower-limb prosthesis. Chapter 6 discusses the design of the experimental setup and chapter 7 presents the conclusions and the future course for carrying this work forward.

CHAPTER 2

Methodology

2.1 Perfect spring balancing with child-parent connections

The first attempt was to perfectly balance an open two-link kinematic chain connected by revolute joints with child-parent spring connections as shown in Figure 2.1.

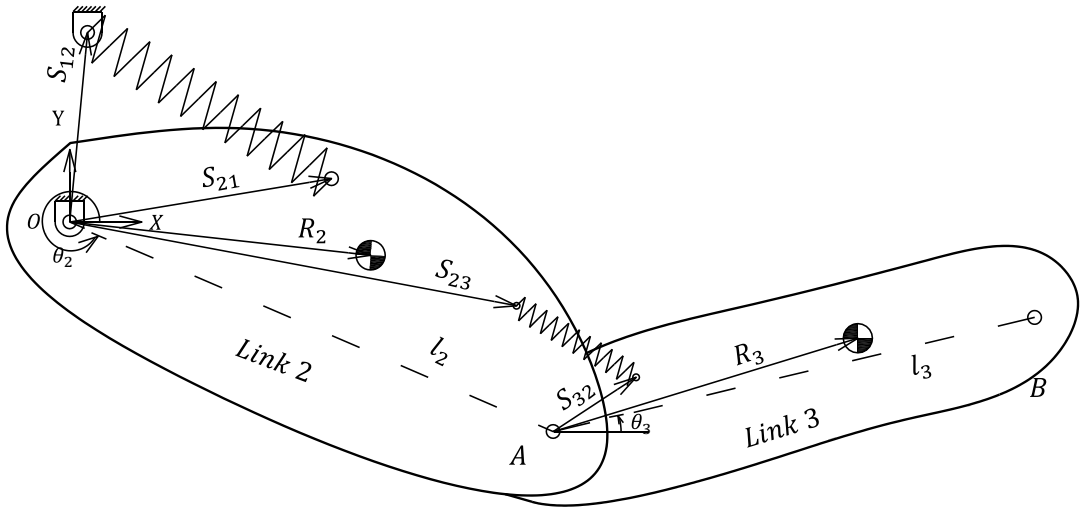

Figure 2.1: Two-link open kinematic chain

Zero-free-length springs are assumed in this section, for the sake of simplifying the proof. The total potential energy of the system is given by

$$\begin{aligned} PE =& m_2 g r_2 \sin(\theta_2 + \alpha_2) + m_3 g[r_3 \sin(\theta_3 + \alpha_3) + l_2 \sin\theta_2] \\ &+ \frac{1}{2} K_1 (\|\mathbf{S}_{21} - \mathbf{S}_{12}\|^2) + \frac{1}{2} K_2 (\|\mathbf{S}_{23} - \mathbf{S}_{32}\|^2). \end{aligned} \tag{2.1}$$

Expanding and simplifying, we get

$$\begin{aligned} PE =& m_2 g r_2 \sin(\theta_2 + \alpha_2) + m_3 g [r_3 \sin(\theta_3 + \alpha_3) + l_2 \sin\theta_2] \\ &+ \frac{1}{2} K_1 [\|\mathbf{S}_{12}\| + \|\mathbf{S}_{21}\|^2 \\ &\qquad - 2 \|\mathbf{S}_{12}\| \|\mathbf{S}_{21}\| \cos(\theta_2 + \beta_{21} - \beta_{12})] \\ &+ \frac{1}{2} K_2 [\|\mathbf{S}_{23}\| + l_2^2 + \|\mathbf{S}_{32}\|^2 \\ &\qquad + 2 l_2 \|\mathbf{S}_{32}\| \cos(\theta_3 - \theta_2 + \beta_{32}) \\ &\qquad - 2 l_2 \|\mathbf{S}_{23}\| \cos\beta_{23} \\ &\qquad - 2 \|\mathbf{S}_{32}\| \|\mathbf{S}_{23}\| \cos(\theta_3 - \theta_2 + \beta_{32} - \beta_{23})]. \end{aligned} \tag{2.2}$$

The potential energy is only a function of θ_2 and θ_3 as all the other quantities are constants. If spring balancing has to be exact, then,

$$\nabla(PE) = \begin{bmatrix} \frac{\partial(PE)}{\partial\theta_2} \\ \frac{\partial(PE)}{\partial\theta_3} \end{bmatrix} = \begin{bmatrix} 0 \\ 0 \end{bmatrix} \tag{2.3}$$

for all θ_2 and θ_3. This implies that

$$\begin{aligned} \frac{\partial(PE)}{\partial\theta_2} =& m_2 g r_2 \cos(\theta_2 + \alpha_2) + m_3 g l_2 \cos\theta_2 \\ &+ K_1 \|\mathbf{S}_{12}\| \|\mathbf{S}_{21}\| \sin(\theta_2 + \beta_{21} - \beta_{12}) \\ &+ K_2 l_2 \|\mathbf{S}_{32}\| \sin(\theta_3 - \theta_2 + \beta_{32}) \\ &- K_2 \|\mathbf{S}_{32}\| \|\mathbf{S}_{23}\| \sin(\theta_3 - \theta_2 + \beta_{32} - \beta_{23}) = 0, \end{aligned} \tag{2.4}$$

and

$$\begin{aligned} \frac{\partial(PE)}{\partial\theta_3} =& m_3 g r_3 \cos(\theta_3 + \alpha_3) \\ &- K_2 l_2 \|\mathbf{S}_{32}\| \sin(\theta_3 - \theta_2 + \beta_{32}) \\ &+ K_2 \|\mathbf{S}_{32}\| \|\mathbf{S}_{23}\| \sin(\theta_3 - \theta_2 + \beta_{32} - \beta_{23}) = 0, \end{aligned} \tag{2.5}$$

Solving these two equations for K_1 and K_2, we get,

$$K_1 = \frac{-[m_2 g r_2 \cos(\theta_2+\alpha_2) + m_3 g l_2 \cos\theta_2 + m_3 g r_3 \cos(\theta_3+\alpha_3)]}{\|\mathbf{S}_{12}\|\|\mathbf{S}_{21}\| \sin(\theta_2+\beta_{21}-\beta_{12})}. \tag{2.6}$$

$$K_2 = \frac{m_3 g r_3 \cos(\theta_3+\alpha_3)}{l_2\|\mathbf{S}_{32}\| \sin(\theta_3-\theta_2+\beta_{32}) - \|\mathbf{S}_{32}\|\|\mathbf{S}_{23}\| \sin(\theta_3-\theta_2+\beta_{32}-\beta_{23})}. \tag{2.7}$$

Let

$$C_1 = \frac{\cos(\theta_2 + \alpha_2)}{\sin(\theta_2 + \beta_{21} - \beta_{12})}, \tag{2.8}$$

$$C_2 = \frac{\cos\theta_2}{\sin(\theta_2 + \beta_{21} - \beta_{12})}, \tag{2.9}$$

and

$$C_3 = \frac{\cos(\theta_3 + \alpha_3)}{\sin(\theta_2 + \beta_{21} - \beta_{12})}. \tag{2.10}$$

Assume the case in which θ_2 is kept constant but θ_3 is varied. Since C_1 and C_2 depend only on θ_2, they remain constant, but C_3 varies; therefore, K_1 varies (Equation 2.6). Hence, K_1 is not constant for all $\{\theta_2,\theta_3\}$ in space where θ_2 and θ_3 are independent of each other.

The basis set of this workspace is $\{\theta_2, \theta_3\}$. The basis can also be taken as $\{\theta_3 - \theta_2, \theta_3\}$ since these two quantities are also linearly independent and the dimension of the workspace remains the same. If we keep $(\theta_3 - \theta_2)$ constant and vary only θ_3, the denominator of Equation 2.7 remains constant, but the numerator varies. Hence, K_2 cannot remain constant over the entire workspace.

Using this argument we show that exact spring balancing with springs of invariant spring constants is impossible over an entire configuration space using serial child-parent connections.

2.2 General Formulation of the Optimization

Balancing implies that the potential energy of the system is made invariant over the configuration space. For a conservative field, the torque, $\tau = -\nabla(PE)$ (for static balancing, the kinetic energy, $(KE) = 0$). In the case of gravity balancing using springs, both the gravitational and spring forces are conservative in nature; hence, this relation is applicable.

By using a spring for static balancing, the net potential energy of the system is made to remain constant,i.e. $\nabla(PE) = 0$, for all domain values of the configuration space variables. The spring stores energy when gravitational potential energy reduces, and it releases energy when gravitational potential energy of the system increases. If perfect spring balancing is not possible, approximate spring balancing can be achieved by minimizing the variance of potential energy over the configuration space.

Let **x** be the vector representing the configuration space variables and **y** be all the design parameters that can be altered such as the spring free length, locations of attachment points of the spring, etc. K_i represents the spring constant of the spring connecting

the ith + 1 child link to its parent, the ith link. The fixed link is the first link. Then,

$$PE = f(\mathbf{x}, \mathbf{y}, K_1, K_2, ..., K_n). \tag{2.11}$$

For each set of $A = (\mathbf{y}, K_1, K_2, ..., K_n)$, the PE at every **x** in space is found. Let the set of all the PE for a particular A be PE_A. The optimization is set up as follows.

$$\begin{aligned} \text{Objective Function :} \quad & variance(PE_A) \\ \text{Control Variable :} \quad & A \\ \text{Compulsory Constraint :} \quad & K_i \geq 0 \text{ for all } i = 1, ..., n \end{aligned} \tag{2.12}$$

Variance stands for the statistical parameter defined as

$$Variance\ (\sigma^2) \ = \ \frac{\sum_{i=1}^{i=n}(x_i - \bar{x})^2}{n-1},$$

where $\bar{x}$ is the average of n data points and x_i is the ith data point.

Apart from the compulsory constraint on K_i, other constraints based on the specific design case can be incorporated.

2.3 Formulation of optimization for specific mechanisms

We start with the classic case of balancing of a single link.

2.3.1 Single Link pivoted to the ground

2.3.1.1 Single link with zero-free-length springs

The configuration for this case is similar to the single link balancing by Rahman *et al.* (1995) (see Figure 2.2).

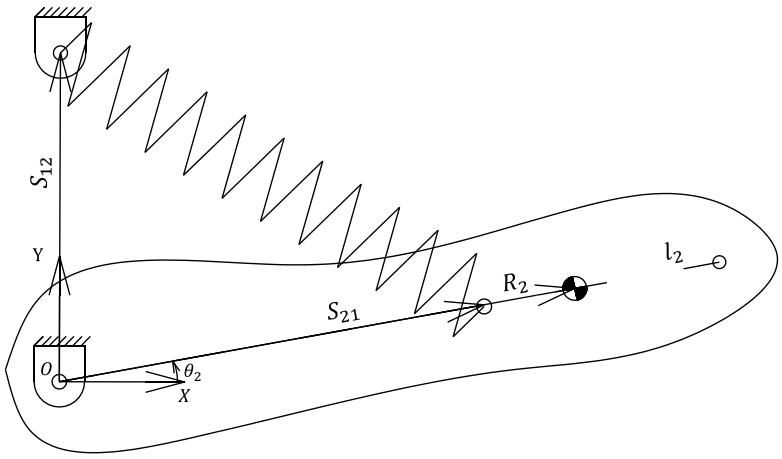

Figure 2.2: Schematic showing balancing a single link (adapted from Rahman *et al.* (1995))

The PE in terms of θ_2 is expressed as

$$PE = m_2 g r_2 \sin(\theta_2 + \alpha_2) + \frac{1}{2} K_1 (\|S_{21} - S_{12}\|^2). \tag{2.13}$$

The parameter values, $\beta_{12} = 90^{\text{o}}$, $\beta_{21} = 0^{\text{o}}$ and $\alpha_2 = 0^{\text{o}}$ are chosen to match the configuration provided by Rahman *et al.* (1995) in their work. $m_2 = 1$kg, $r_2 = 0.25$m, $\|S_{12}\| = 0.1$m and $\|S_{21}\| = 0.2$m were chosen randomly.

An optimization problem was formulated according to Equation 2.12 with the PE given by Equation 2.13 and K_1 as the only control variable. The optimization was performed using MATLAB®'s optimization toolbox (Grace and Works (1990)). The function fmincon was used for this particular optimization. The result of the optimization gave

$$K_1 = 122.5012\ N/m \text{ by PE variance minimization.}$$

According to Rahman *et al.* (1995), for perfect spring balancing,

$$K_1 = \frac{m_2 g r_2}{\|S_{12}\|\,\|S_{21}\|} = 122.5\ N/m.$$

Thus, the spring constant obtained by optimization closely matches with the exact solution for the single-link case.

2.3.1.2 Single link with non-zero-free-length springs

For this case, we introduce a non-zero-free-length spring with free length len in place of the zero-free-length-spring in Figure 2.2. Previous work by Rahman *et al.* (1995)

has shown that exact balancing is not possible with a single non-zero-free-length spring connected in the manner shown in figure 2.2. The potential energy can be expressed as

$$PE = m_2 g r_2 \sin(\theta_2 + \alpha_2) + \frac{1}{2} K_1 (\|S_{21} - S_{12}\| - len)^2. \tag{2.14}$$

According to the general formulation in Section 2.2, $x = \theta_2$; $A = \begin{bmatrix} len \\ K_1 \end{bmatrix}$. Apart from the compulsory constraint on K_1 (Section 2.2), another constraint is introduced: $len \geq 0.05$m, that is, the free length of the spring should be greater than or equal to 5 cm. Performing the optimization, we get

$$A = \begin{bmatrix} 0.05\ m \\ 161.39\ N/m \end{bmatrix}.$$

The spring balancing thus obtained is not exact, but reduces the torque requirement of the system considerably. Figure 2.3 shows the potential energy distribution over the configuration space for the unbalanced link, perfect balancing and approximate balancing. Table 2.1 shows the peak actuator requirements before and after approximate balancing. Figure 2.4 gives a comparison of the actuation torque values before and after balancing. Note that the torque requirement would be zero for perfect balancing.

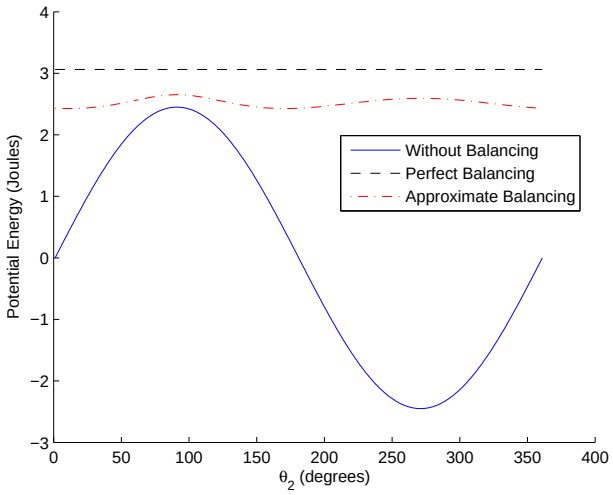

Figure 2.3: Plot of Potential Energy distribution over space(θ_2) for a single link

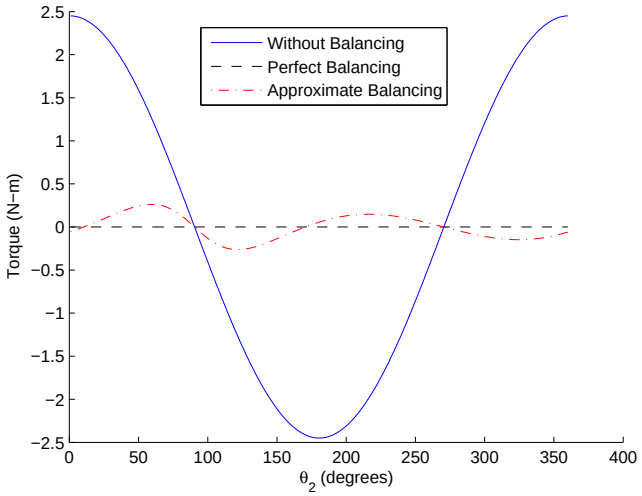

Figure 2.4: Plot of the actuator torque requirement for an unbalanced, perfectly-balanced and approximately-balanced single link

Table 2.1: Peak actuator torque for single link with and without approximate balancing

Actuator	Unbalanced peak torque (Nm)	Balanced peak torque (Nm)	Torque reduction
1	2.45	0.23	90.5%

2.3.1.3 Incorporating additional design parameters for optimization

For the sake of simplicity, only the spring constants and free length of the springs were used as control variables, with the other parameters kept constant. However, the method for approximate balancing described in this work is very flexible. For example, the position of the spring pivots, S_{ij} can be included in the control variables so that,

$$A = \begin{bmatrix} \|S_{ij}\| \\ \beta_{ij} \\ len \\ K \end{bmatrix}.$$

To illustrate, the example in Section 2.3.1.2 is extended to include more design parameters. The control variables now include the position of the spring pivot, and therefore, $A = \begin{bmatrix} \|S_{21}\| \\ len_1 \\ K_1 \end{bmatrix}$. In addition to the earlier constraints, a new constraint is added to keep the pivot point of the spring on the link within some desired range, say,

$$0.05\ m \leq \|S_{21}\| \leq 0.5\ m.$$

Potential energy variance minimization yields

$$A = \begin{bmatrix} 0.294\ m \\ 0.05\ m \\ 99.96\ N/m \end{bmatrix}.$$

The optimization using these values yields a peak torque for the actuator of 0.10 Nm which is lower than the earlier value of 0.23 Nm (see Figure 2.5 and Table 2.1). This is as expected since more parameters are included as control variables in the optimization problem. However, the optimization problem can become very complex when more control variables and constraints are involved. Normal gradient-based methods lead to local convergence here. Heuristic optimization methods may be more appropriate in this scenario for greater likelihood of global convergence. Using a genetic algorithm consumes a lot of time and computational effort, hence, simulated annealing was ran two or three times and the obtained minima was used as a guess value for a gradient based method using the function fmincon in Matlab optimization toolbox. The best of those solutions was picked as the minima.

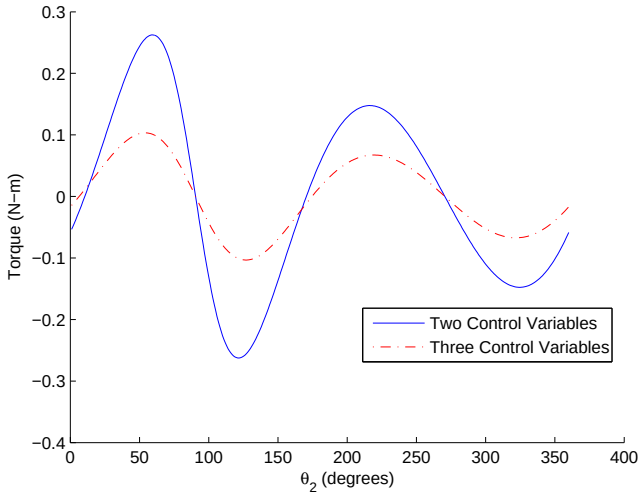

Figure 2.5: Plot of torque with extra design variable for the case in section 2.3.1.2

2.3.2 Generalized formulation for an n-link open kinematic chain

The formulation of potential energy variance minimization can be extended to the case of an open kinematic chain with n links (excluding ground) connected by revolute

joints. Figure 2.6 shows an open kinematic chain with n links. The basis of the configuration space has n elements $\{\theta_2, \theta_3, ..., \theta_{n+1}\}$ corresponding to the n degrees of freedom.

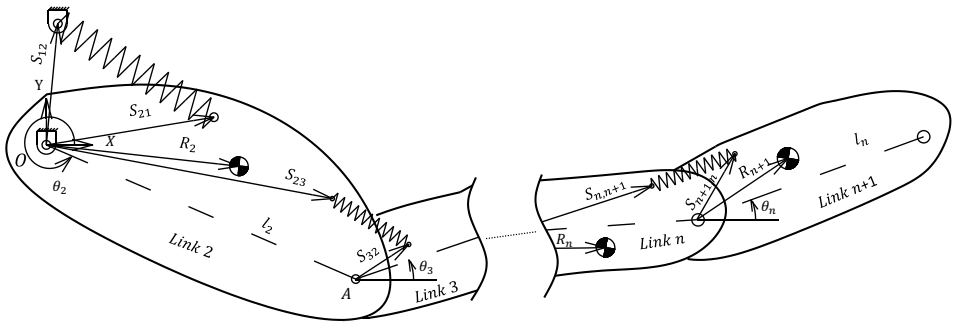

Figure 2.6: Illustrative schematic of an n-link (excluding ground) open kinematic chain

Each degree of freedom is controlled by an actuator. Let actuator (j) control θ_{j+1}. To reduce the actuator requirement for actuator j, the potential energy variance must be minimized for all the links ahead of it, that is, for links $(j+1)$ to n. The potential energy to be used for actuator j is represented by

$$\begin{aligned} PE^j = \sum_{i=j+1}^{i=n+1} & [m_i g r_i \sin(\theta_i + \alpha_i) \\ & + \frac{1}{2} K_{i-1}(\|S_{i,i-1} - S_{i-1,i}\| - len_{i-1})^2]. \end{aligned} \tag{2.15}$$

Variance($PE^j_{A_j}$) is minimized starting from the distal part of the linkage, that is, from actuator n. The optimization yields A_n. We then optimize for actuator $(n-1)$ using A_n to get A_{n-1}. The process is repeated until A_1 is obtained.

2.3.3 Formulation for a fourbar linkage

The most common example of a closed-loop kinematic chain is a four-bar linkage. In this section, the method of PE variance minimization is applied to a four-bar linkage, which has four links including the ground. The nomenclature used is the same as that for an n-link open chain. Here, the number of links excluding ground is 3. This optimization technique will work for any number of springs connected between any two bodies. For the sake of simplicity, two springs are considered - one each between the

non-floating links and the ground, as shown in Figure 2.7.

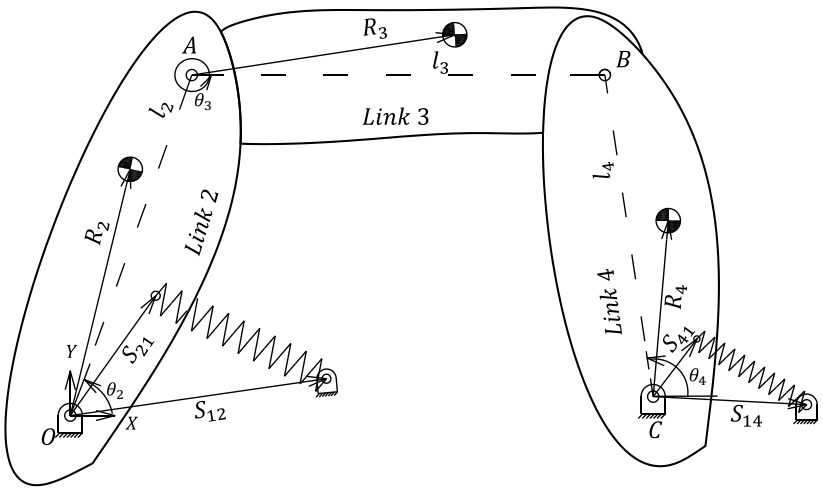

Figure 2.7: Schematic showing the balancing a general four-bar linkage

Since a fourbar is a one-degree-of-freedom (DOF) mechanism, the basis set has only one element. Let it be $\{\theta_2\}$. Position analysis of the fourbar is performed first to express θ_3 and θ_4 in terms of θ_2. The PE of the system is given by

$$\begin{aligned} PE &= m_2 g r_2 \sin(\theta_2 + \alpha_2) + m_3 g(l_2 \sin\theta_2 + r_3 \sin(\theta_3 + \alpha_3)) \\ &\quad + m_4 g(l_1 \sin\theta_1 + r_4 \sin(\theta_4 + \alpha_4)) \\ &\quad + \tfrac{1}{2} K_1(\|S_{12} - S_{21}\| - len_1)^2 \\ &\quad + \tfrac{1}{2} K_2(\|S_{14} - S_{41}\| - len_2)^2. \end{aligned} \tag{2.16}$$

Potential energy variance minimization is set up as outlined in Section 2.2. In the 1-DOF fourbar with θ_2 as input, K_1 and K_2 can be found simultaneously as only θ_2 is controlled by an actuator.

2.3.4 Formulation for spatial open chain mechanisms

The spring balancing technique proposed in this work has been extended to the balancing of spatial open chain mechanisms as well. The formulation of the optimization problem remains similar to that for planar mechanisms, and Denavit-Hartenberg (D-H) parameters are used to compute kinematics of spatial mechanisms. See figure 2.8. Coordinate systems o_0 and o_1 are both fixed and do not move. Z_1 is aligned according to the axis of the rotary actuator 1. This may not be in the vertical direction always. Height of the centre of mass of the links is what is required for calculation of the potential energy, hence, the coordinate system 0 was introduced to take care of it.

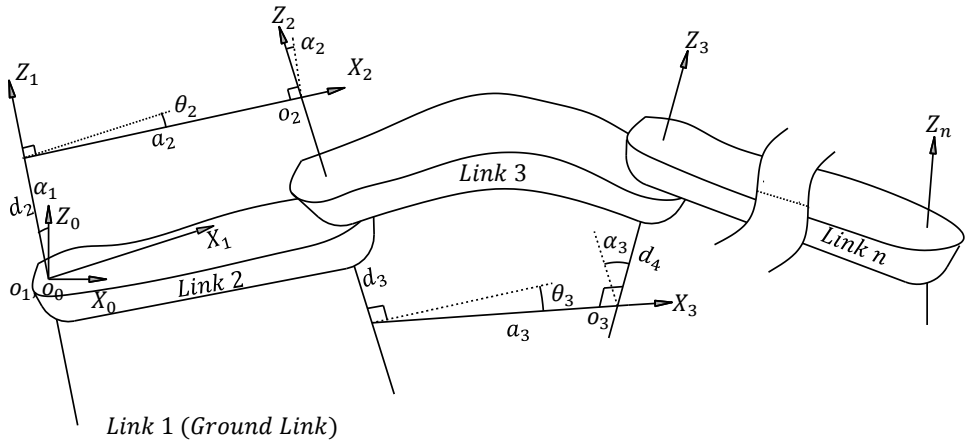

Figure 2.8: Schematic showing D-H parameter convention

As before, the total potential energy of the links for the entire workspace is written and the variance is found out which is minimized to obtain spring characteristics.

In this section any vector V is written in the homogeneous form, i.e.,

$$V = \begin{bmatrix} x \\ y \\ z \\ 1 \end{bmatrix} \tag{2.17}$$

The transformation matrix from i^{th} coordinate system to $(i-1)^{th}$ is written as

$$T_i^{i-1} = \begin{bmatrix} \cos(\theta_i) & -\sin(\theta_i)\cos(\alpha_i) & \sin(\theta_i)\sin(\alpha_i) & a_i\cos(\theta_i) \\ \sin(\theta_i) & \cos(\theta_i)\cos(\alpha_i) & -\cos(\theta_i)\sin(\alpha_i) & a_i\sin(\theta_i) \\ 0 & \sin(\alpha_i) & \cos(\alpha_i) & d_i \\ 0 & 0 & 0 & 1 \end{bmatrix} \forall i \geq 2 \tag{2.18}$$

0^{th} coordinate system is the fixed frame of reference, whereas all others are moving coordinate systems.

$$T_1^0 = \begin{bmatrix} \cos(\alpha_i) & 0 & \sin(\alpha_i) & 0 \\ 0 & 1 & 0 & 0 \\ -\sin(\alpha_i) & 0 & \cos(\alpha_i) & 0 \\ 0 & 0 & 0 & 1 \end{bmatrix} \tag{2.19}$$

$$PE^j = \sum_{i=j+1}^{i=n+1} \left[m_i g r_i^z + \frac{1}{2} K_{i-1} (\left\| T_i^{i-1} S_{i,i-1} - S_{i-1,i} \right\| - len_{i-1})^2 \right]. \tag{2.20}$$

$$R_i^0 = T_i^0 R_i^i \tag{2.21}$$

$$T_i^0 = T_1^0 T_2^1 T_3^2 .....T_i^{i-1} \tag{2.22}$$

$$r_i^z = R_i^0(3,1) \tag{2.23}$$

Variance($PE^j_{A_j}$) is minimized starting from the distal part of the linkage, that is, from actuator n. The optimization yields A_n. We then optimize for actuator $(n-1)$ using A_n to get A_{n-1}. The process is repeated until A_1 is obtained.

In this chapter we argued that perfect spring balancing with springs of invariant spring constants using child-parent connections of a two-link arm is not possible. A method is proposed to accomplish approximate spring balancing and presented in a generalized manner. This method is formulated for planar open chain linkages, planar spatial linkages and a four-bar mechanism. Potential energy variance minimization method is the core of this entire work. In the further chapters we will apply this method to various examples and look deeply into the case of lower-limb balancing.

CHAPTER 3

Design examples using approximate spring balancing

In this section, the PE variance minimization method is used to design for gravity balancing of a lower-limb orthosis (example of an open kinematic chain), a manually-operated sit-to-stand wheelchair mechanism (closed kinematic chain), spatial single link and spatial two link kinematic chains.

3.1 Approximate balancing of a two-link lower-limb orthosis

A lower-limb orthosis is a supportive device to enable users with weakened leg muscles (due to various pathologies such as post-polio, spinal cord injury, cerebral palsy, etc.) to walk. Gravity balancing is of tremendous importance for this application since users typically have limited muscular capabilities and the device adds additional weight. Agrawal and Agrawal (2005) present a design for a lower-limb orthosis using static balancing with springs and auxiliary links. We redesign the orthosis with the new methodology in this section. The moveable (with respect to a stationary pelvis) links considered are the femoral and tibial links, so $n = 2$. The relevant values for the various parameters were taken from Agrawal and Agrawal (2005). The parameters used are:

$$r_2 = 0.177 \text{ m}, r_3 = 0.185 \text{ m}, l_2 = 0.432 \text{ m},$$
$$\alpha_2 = 0^{\text{o}}, \alpha_3 = 0^{\text{o}}, \beta_{21} = 0^{\text{o}}, \beta_{12} = 90^{\text{o}}, \beta_{23} = 0^{\text{o}}, \beta_{32} = 0^{\text{o}},$$
$$m_2 = 7.39 \text{ kg}, m_3 = 4.08 \text{ kg}, g = 9.8 \text{ m/s}^2,$$
$$240^{\text{o}} \leq \theta_2 \leq 300^{\text{o}}, \text{ and } (\theta_2 - 60^{\text{o}}) \leq \theta_3 \leq \theta_2$$

The attachment points of the springs were also selected as a part of the control variables for optimal placement of the springs. The constraints placed on this optimization were -

1. Maximum length of the spring should be less than 1.5 times its free length to make sure that the spring is within its feasible range of operation

2. Minimum length of the spring should be greater than the free length of the spring to ensure that a tension spring is obtained

3. Spring constant should be greater than 0 and less than 10000 N/m

The potential energy variance(PE^2_{A2}) is minimized subject to the constraints specified above to obtain A_2:

$$A_2 = \begin{bmatrix} K_2 \\ len_2 \\ \|S_{23}\| \\ \|S_{32}\| \end{bmatrix} = \begin{bmatrix} 1128 \text{ N/m} \\ 0.18 \text{ m} \\ 0.26 \text{ m} \\ 0.1 \text{ m} \end{bmatrix}$$

Using A_2, the PE variance(PE^1_{A1}) is minimized subject to the constraints to obtain A_1 as:

$$A_1 = \begin{bmatrix} K_1 \\ len_1 \\ \|S_{12}\| \\ \|S_{21}\| \end{bmatrix} = \begin{bmatrix} 2000 \text{ N/m} \\ 0.31 \text{ m} \\ 0.19 \text{ m} \\ 0.26 \text{ m} \end{bmatrix}$$

Gradient-based methods failed to give a global convergence; hence a genetic algorithm was used for this optimization using the MATLAB® optimization toolbox (Grace and Works (1990)).

Table 3.1: Comparison of results of hip and knee joint torques between balanced and unbalanced cases

Actuator	Unbalanced	Balanced	Torque reduction	
	torque (Nm)	torque (Nm)	Optimization	Agrawal(2005)
1 (Hip Joint)	22.24	6.44	71.0%	90%
2 (Knee Joint)	7.41	3.70	50.0%	50%

Table 3.1 shows the torques obtained using minimization of the PE variance and compares the reduction to the values reported in Agrawal and Agrawal (2005). The torque reduction by the proposed method is lower than the torque reduction by the method used in Agrawal and Agrawal (2005), but the PE variance minimization technique eliminates the need for auxiliary links making the entire mechanism compact and more practical. More parameters such as β's of the spring pivot positions can also be varied. See Figures 3.1 and 3.2 for torque variation with (θ_2, θ_3) before and after spring balancing.

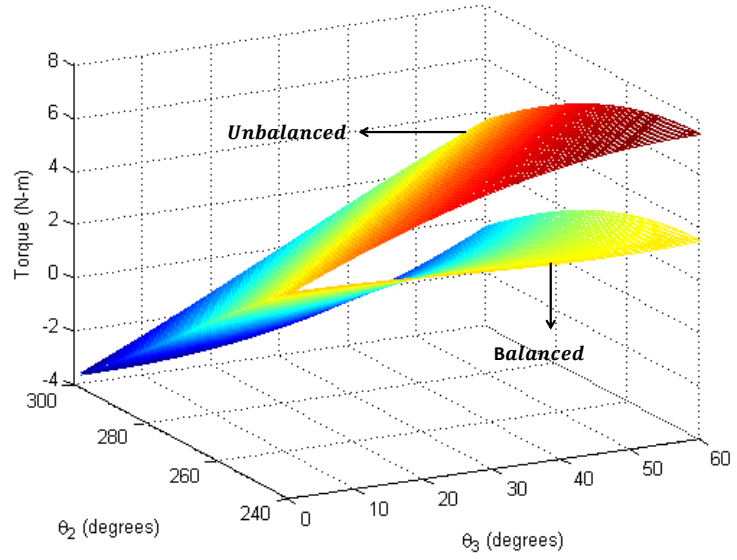

Figure 3.1: Plot of torque for actuator 2 (knee joint) before and after spring balancing

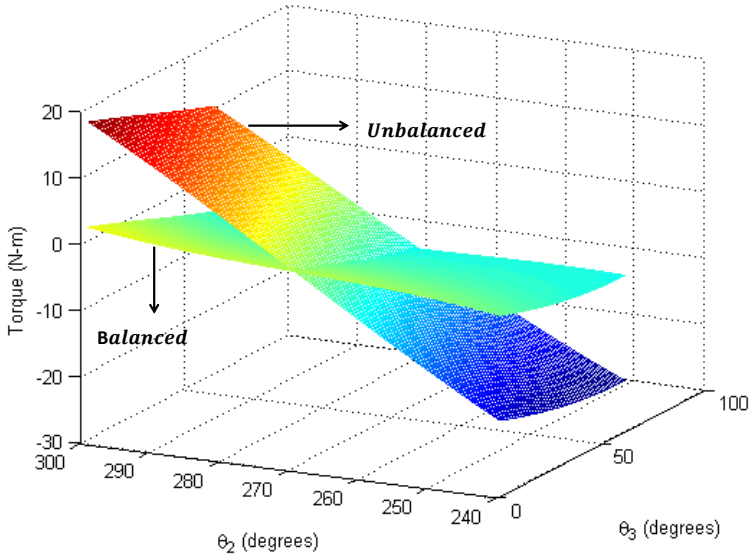

Figure 3.2: Plot of torque for actuator 1 (hip joint) before and after spring balancing

Actual springs were designed for spring 1 and 2 using Norton (1996). The extension springs so obtained are made of music wire, a commonly used material for springs, and are neither too bulky nor too heavy. Table 3.2 presents the parameters of the spring design for the two springs used in the orthosis.

Table 3.2: Spring design for lower-limb orthosis

Spring	Spring constant (N/m)	Wire diameter (mm)	Coil diameter (mm)	Number of turns	Mass (kg)
1	2000	4	26	76	0.600
2	1128	3	23	60	0.238

A schematic of the lower body orthosis was modeled (Figure 3.3) to visualize the practical space requirement of the designed springs. Note that the direct use of zero-free-length-springs and the absence of auxiliary links and systems to simulate non-zero-free-length springs makes this design less complex and more cost-effective.

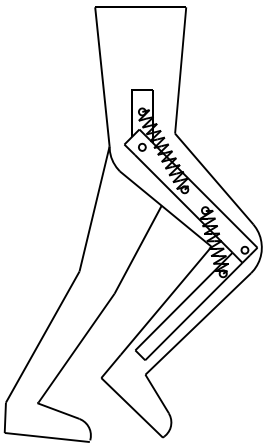

Figure 3.3: A schematic of the orthosis with the designed springs, modeled to scale

3.2 Fourbar example: Balancing of a sit-to-stand wheelchair

Reducing actuator loads is also important for applications in which human effort is required for actuation. A manually-powered sit-to-stand wheelchair developed in the Rehabilitation Research & Device Development (R2D2) Lab in IIT Madras uses a four-bar mechanism actuated by the user through a driver dyad [Chaudhari (2012)]. Actuator torque minimization is critical since the user has to lift himself/herself from the sitting to the standing position using his/her upper body strength. Balancing by the potential energy variance minimization method for a four-bar linkage was applied to this design problem. The mechanism accomplishing the sit-to-stand motion of the wheelchair is a parallelogram linkage (a-b-c-d) as shown in Figure 3.4 adapted from Chaudhari (2012).

An extension spring was designed to be connected between a-c to utilize the unused space below the seat.

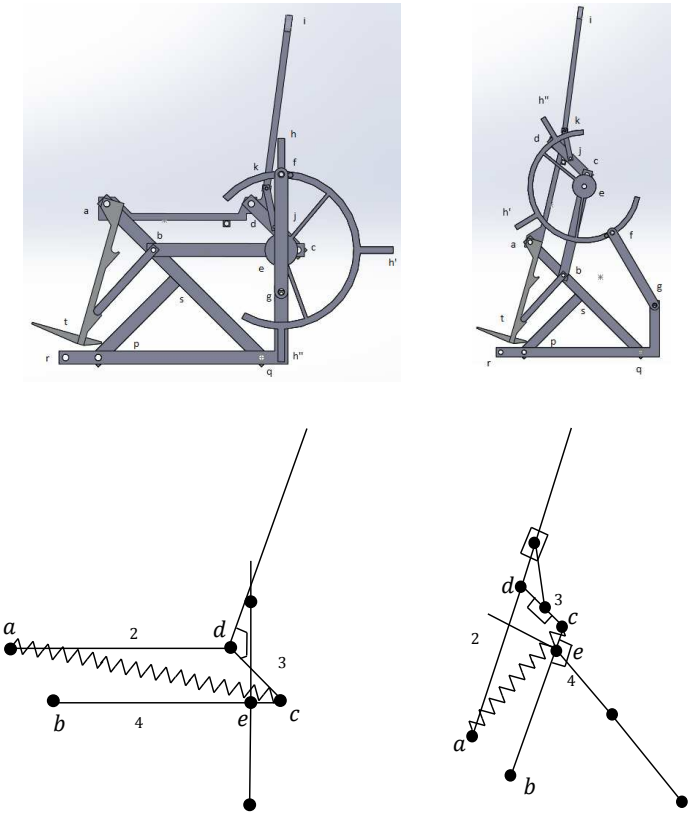

Figure 3.4: Schematic illustrating the mechanism of sit-to-stand wheelchair(adapted from Chaudhari (2012))

The PE for the four-bar parallelogram linkage is given by

$$\begin{aligned} PE &= m_2 g r_2 \sin(\theta_2 + \alpha_2) + m_3 g(l_2 \sin\theta_2 + r_3 \sin(\theta_3 + \alpha_3)) \\ &\quad + m_4 g(l_1 \sin\theta_1 + r_4 \sin(\theta_4 + \alpha_4)) \\ &\quad + \frac{1}{2} K_1 (\|S_{13} - S_{31}\| - len_1)^2 \end{aligned} \tag{3.1}$$

The configuration space for this application is $0^o \leq \theta_2 \leq 85^o$. The sit-to-stand device is designed for a person weighing 100 kg. The relevant parameters related to the design are taken from Chaudhari (2012):

$$m_2 = 103 \text{ kg}, m_3 = 1.5 \text{ kg}, m_4 = 3 \text{ kg}$$
$$l_1 = 200 \text{ mm}, l_2 = 440 \text{ mm}, l_3 = 200 \text{ mm}, l_4 = 440 \text{ mm}$$
$$r_2 = 220 \text{ mm}, r_3 = 100 \text{ mm}, r_4 = 220 \text{ mm},$$

$$g = 9.8\ m/s^2, \theta_1 = 315^{\circ}.$$

The control variables are $A = \begin{bmatrix} len1 \\ K_1 \end{bmatrix}$. Apart from the compulsory constraint on K_1 to ensure that the spring is always in tension, the free length must be less than the minimum length of the spring during operation. $len1 \leq min(\|S_{13} - S_{31}\|) = 0.3642$ m and $len_1 \geq 0.1$ m. Minimizing variance(PE_A) subject to the specified constraints results in

$$A = \begin{bmatrix} 0.364\ m \\ 6902\ N/m \end{bmatrix}.$$

Since the parallelogram is actuated by a dyad, the force analysis was done using ADAMS®. Figures 3.5 and 3.6 show the torque requirement without and with balancing, respectively. This is the torque the user has to apply at joint e to lift himself/herself from sitting to the standing position (see Figure 3.4).

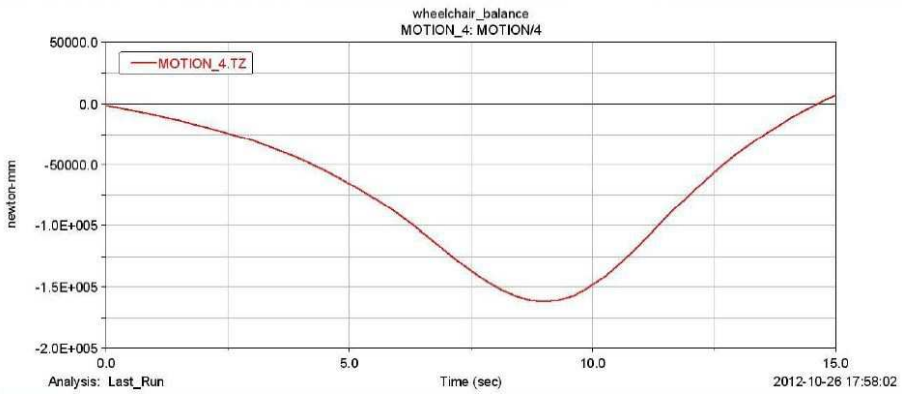

Figure 3.5: Plot of wheelchair actuation torque before balancing

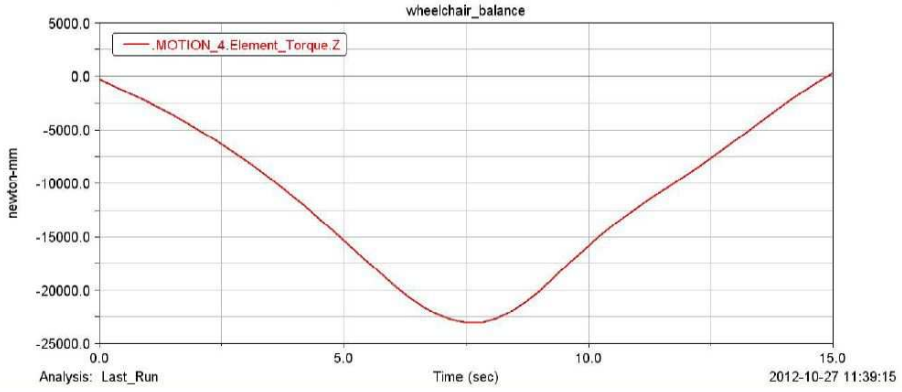

Figure 3.6: Plot of wheelchair actuation torque after balancing

The torque required to actuate the linkage before and after spring balancing are compared in Table 3.3.

Table 3.3: Comparison of results for wheelchair before and after balancing

Torque before balancing (Nm)	Torque after balancing (Nm)	Torque reduction
160	23	85.62%

The results obtained after optimization were used to design a usable spring using Norton (1996). There are two mechanisms, one on either side of the wheelchair and hence two springs are required. Therefore, the spring constant for the spring design is taken as half of the value obtained by optimization. The material used is music wire and the parameters of the spring designed are specified in Table 3.4.

Table 3.4: Spring design for sit-to-stand wheelchair

Spring Constant	Wire Diameter	Coil Diameter	No. of Turns	Mass
3451 N/m	6 mm	40 mm	61.5	1.65 kg

3.3 Spatial link balancing

3.3.1 Single link on a pivot

A single link is pivoted about a z-axis. The angle of the pivot axis, i.e. z with the vertical is defined as α, in accordance with D-H parameter convention. Following relevant parameters of the link were considered

$$m_2 = 2kg,\ a_2 = 0.3m,\ d_2 = 0m,\ \alpha_1 = 30^{\circ},\ \alpha_2 = 0^{\circ}$$

$$R_2 = \begin{bmatrix} -0.1m \\ 0 \\ 0 \\ 1 \end{bmatrix}, S_{12} = \begin{bmatrix} 0 \\ 0 \\ 0.05m \\ 1 \end{bmatrix}, S_{21} = \begin{bmatrix} -0.2m \\ 0 \\ 0 \\ 1 \end{bmatrix}$$

Here S_{21} and R_2 are written with respect to the moving coordinate system 2 on the link. Refer Figure 2.8.

Potential energy variance minimization was performed. See figure 3.7 (left) for potential energy distribution at $\alpha_1 = 30^o$. The K obtained was 784 N/m.

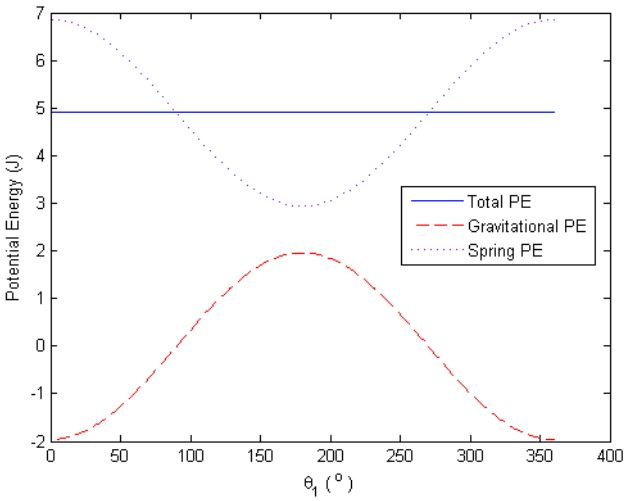

Figure 3.7: Plot of Potential Energy distribution for spatial single link balancing with a zero free length spring

An interesting result to note here was that keeping everything constant and just varying α_1, the spring constant obtained was always 784 N/m for perfect balancing apart from the case of $\alpha_1 = 0$. For $\alpha_1 = 0$ the link rotates in a horizontal plane, hence, physically there is no meaning of spring balancing in that case. The fact that for all other α_1 the spring constant remains same can be exploited to reduce the computations required for balancing of a link with a ball and socket joint. The number of computations would go down from n^3 to n as we can reduce the case of a ball and socket joint to a simple single link pivoted to the ground.

This was followed by balancing of of the same single spatial link with a spring of non-zero free length. In this case the α_1 was taken as 45^o. The free length of the spring was constrained between 0.075m to 0.15m. A for this optimization was

$$A = [K \ len]^T \tag{3.2}$$

The minima obtained was

$$A_{min} = [2483\,\mathrm{N/m}\ 0.075\mathrm{m}]^T \tag{3.3}$$

The peak torque on doing so reduced from 2.77 Nm to 1.17 Nm, i.e. a peak torque reduction of 57.7 %. See Figure 3.8 for comparison of torque distribution over the entire workspace of the link in balanced and unbalanced state.

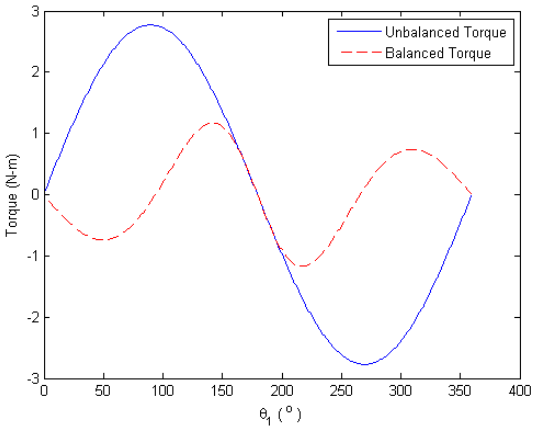

Figure 3.8: Plot of torque comparison between an unbalanced and balanced spatial link

3.3.2 Two link balancing

Using potential energy variance minimization, a spatial two link two DOF manipulator was balanced. The relevant mechanism parameters were

$$m_2 = 2 \text{ kg}, m_3 = 2 \text{ kg},$$
$$0.07m \leq len_1, len_2 \leq 0.15m$$
$$\alpha_1 = 90^o, \alpha_2 = 20^o, \alpha_3 = 45^o$$
$$R_2 = \begin{bmatrix} -0.1m \\ 0 \\ 0 \end{bmatrix}, R_3 = \begin{bmatrix} -0.1m \\ 0 \\ 0 \end{bmatrix}$$
$$S_{12} = \begin{bmatrix} 0 \\ 0 \\ 0.05m \end{bmatrix}, S_{21} = \begin{bmatrix} -0.2m \\ 0 \\ 0 \end{bmatrix}, S_{23} = \begin{bmatrix} -0.1m \\ 0 \\ 0 \end{bmatrix}, S_{32} = \begin{bmatrix} -0.2m \\ 0 \\ 0 \end{bmatrix}$$

The minima obtained were

$$A_2 = [715 \,\text{N/m}\ 0.071\text{m}]^T \tag{3.4}$$

$$A_1 = [7464 \,\text{N/m}\ 0.076\text{m}]^T \tag{3.5}$$

See Table 3.5 for results and Figures 3.10 and 3.9 for torque distribution of each link over the workspace.

Table 3.5: Two link spatial manipulator results

Actuator	Unbalanced	Balanced	Torque reduction
	torque (Nm)	torque (Nm)	Optimization
Actuator 1 (proximal)	13.72	3.51	74.4%
Actuator 2 (distal)	3.92	3.56	9.2%

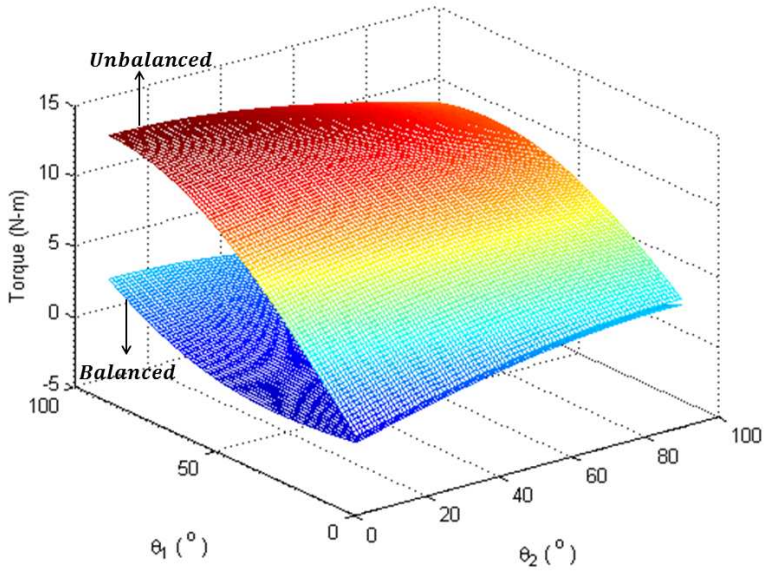

Figure 3.9: Comparison of unbalanced and balanced torque distribution for actuator 1

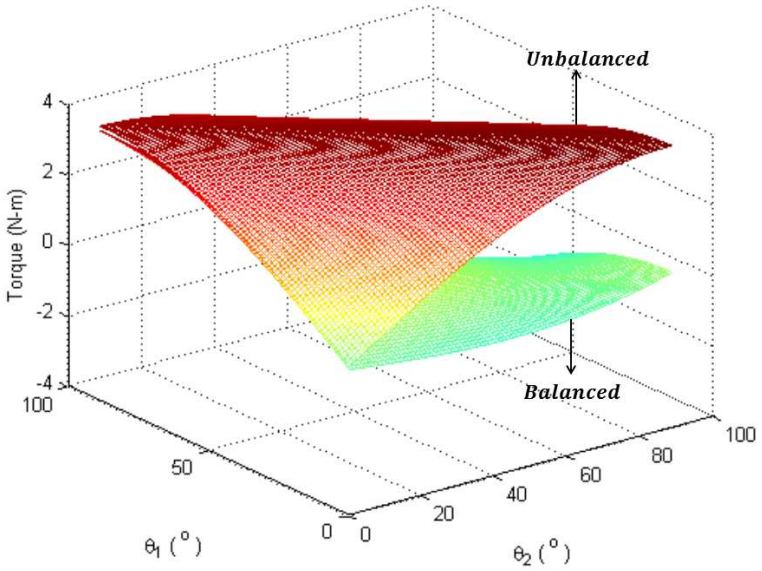

Figure 3.10: Comparison of unbalanced and balanced torque distribution for actuator 2

The small reduction in peak torque for actuator 2 happens as the link approaches a point of singularity in the workspace. At a singularity the force applied by the spring is unable to generate any torque about the actuator making the presence of a spring useless resulting in the value of torque to be same as that of an unbalanced case at the singularity.

In this chapter we saw the results obtained by spring balancing using potential energy variance minimization. The method effectively lowers the torque requirement of the mechanism over the workspace. An important point to note is that the springs designed and their attachment points are dependent on the workspace of the mechanism. When the workspace of the mechanism changes, so do the spring parameters. Uptil this point we have only looked into spring balancing using coil springs. In the next chapter we will extend this method for gas-springs and torsional springs as these two are very common and bear certain advantages over coil springs.

CHAPTER 4

Gas Springs, Torsional Springs and Peak Torque Minimization

4.1 Gas-springs

Gas-springs are extensively used in automobile industry and in many products such as wall folding beds. Compression gas springs and tension gas springs, both are available. Essentially a gas spring is a cylinder filled with compressed gas. See figure 4.1.

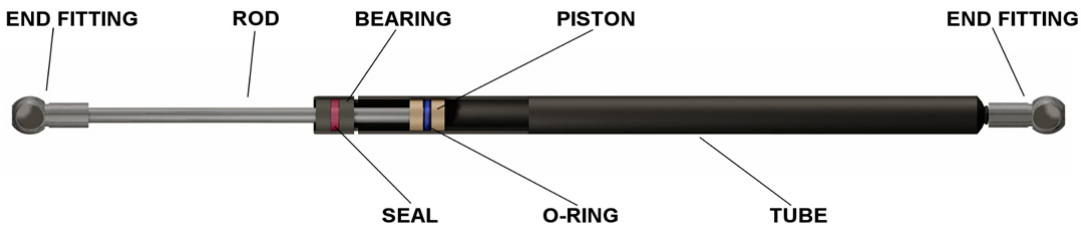

Figure 4.1: Illustrative shematic of a Gas Spring (Figure Courtesy: Titaneps (2012))

When a force is applied on the gas spring, the piston that slides in the cylinder compresses the gas leading to an increase in pressure that causes the force required to move the spring to rise up. The characteristic curve, i.e., force vs deflection curve of a gas spring is a straight line with a positive slope and a positive intercept with the force axis as can be seen on the website of manufacturers SuperGasSprings (2007); Lesjoforbs (2013). There is a difference between the force curve while compressing and extending due to a friction force, but in our work here we have neglected friction for all calculations. Hence, the characteristic curve for compression and extension is same. See figure 4.2

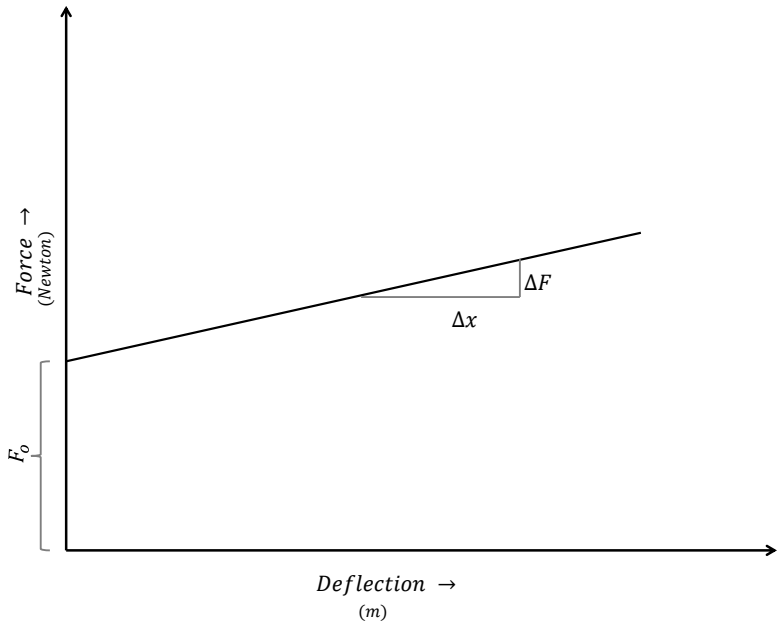

Figure 4.2: Force-deflection characteristic curve

The gas-spring can be seen analogous to a compression or tension spring with a preload force. On deflection from the preload position, the force vs deflection curve would be a straight line with a positive slope. Thus the parameters required to define the force of the gas spring are the preload force (F_o), the slope of the characteristic curve which is same as the spring constant (K) and the amount of deflection.

At this juncture there is a need to clarify the difference between k and K. k also called as k-factor of a gas spring, is widely used in the industry. It is defined as the ratio between the maximum force to the minimum force that can be applied by the gas spring. The K we will use in this section is the spring constant of the gas-spring, i.e., the slope of the characteristic curve.

Thus the potential energy of the spring can be written as,

$$PE = F_o\delta + \frac{1}{2}K\delta^2 \tag{4.1}$$

Balancing using gas-springs

In this section, the use of a gas-spring for balancing a fourbar mechanism is implemented on a manually powered sit-to-stand wheelchair developed in Rehabilitation Research and Device Development lab at IIT-Madras. See figure 4.3.

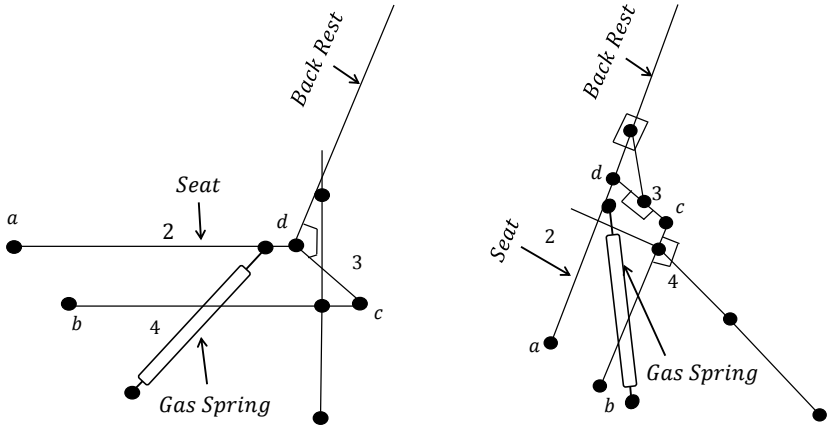

Figure 4.3: Wheelchair with gas-spring in sitting(left) and standing(right)

The total potential energy of the mechanism is written as,

$$\begin{aligned} PE &= m_2 g r_2 \sin(\theta_2) + m_3 g[l_2 \sin\theta_2 + r_3 \sin(\theta_3)] \\ &\quad + m_4 g[l_1 \sin\theta_1 + r_4 \sin(\theta_4)] \\ &\quad + F_o(\|S_{12} - S_{21}\| - len_1) + \frac{1}{2} K_1(\|S_{12} - S_{21}\| - len_1)^2 \end{aligned} \tag{4.2}$$

The variation of the angles of the linkages of the parallelogram mechanism is

$$\begin{aligned} 0^{\text{o}} \leq \quad \theta_2 = \theta_4 \quad &\leq 80^{\text{o}} \\ \theta_3 = 135^{\text{o}} & \end{aligned}$$

Potential energy variance minimization is formulated as described in section 2.2. The set of control variables we have are,

$$A = [F_o \; K \;\; \|S_{12}\| \;\; \beta_{12} \;\; \|S_{21}\|]^T \tag{4.3}$$

The relevant parameters related to the design are taken from Chaudhari (2012):

$$m_2 = 103 \text{ kg}, m_3 = 1.5 \text{ kg}, m_4 = 3 \text{ kg}$$
$$l_1 = 200 \text{ mm}, l_2 = 440 \text{ mm}, l_3 = 200 \text{ mm}, l_4 = 440 \text{ mm}$$
$$r_2 = 220 \text{ mm}, r_3 = 100 \text{ mm}, r_4 = 220 \text{ mm},$$
$$g = 9.8\ m/s^2, \theta_1 = 315^{\text{o}},$$
$$\alpha_2 = 0^{\text{o}}, \alpha_3 = 0^{\text{o}}, \alpha_4 = 0^{\text{o}}$$

Matlab® was used to run the optimization. The result obtained was,

$$A_{min} = [700\text{N}\ 1000\text{N/m}\ 0.3\text{m}\ -69^{\text{o}}\ 0.4\text{m}]^T \tag{4.4}$$

Using Adams® the torque required to go from sitting to standing position was found. The peak torque with the gas-springs was around 8.2 Nm. See figure 4.4.

Figure 4.4: Input moment to move from sitting to standing

Peak torque with tension springs was around 23 Nm, as shown in section 3.2. Gas springs brought down the peak torque 66% below the peak torque for extension springs.

The parameters of the gas spring designed are shown in Table 4.1.

Table 4.1: Design parameters of the gas spring for balancing a standing wheelchair

F_o	Stroke Length	Total Length	Minimum Force	Maximum Force
350 N	318 mm	643 mm	350 N	462 N

4.2 Torsional Springs

The force applied by a torsional spring is directly proportional to the angle of rotation of the spring.

$$F = K\theta \tag{4.5}$$

Hence, the potential energy stored by a torsional spring on rotation by a certain angle θ is

$$PE = \frac{1}{2}K\theta^2 \tag{4.6}$$

These springs occupy very less space and are easier to assemble compared to coil springs. Perfect balancing with torsional springs is not possible because the potential energy is not sinusoidal in nature, hence, it cannot completely eliminate the effect of the sinusoidal variations of the gravitational potential energy, but as mentioned before, due to their lower space requirements they might be handy for certain mechanisms with limited workspace.

The total potential energy for a single link with a torsional spring can be written as,

$$PE = m_2 g r_2 \sin(\theta_2) + \frac{1}{2}K(\theta_2 - \theta_{nat})^2 \tag{4.7}$$

$$90^{\circ} \leq \theta_2 \leq 270^{\circ} \tag{4.8}$$

An optimization is setup as before.

$$A = [K\ \theta_{nat}]^T \tag{4.9}$$

Contrary to expectations, on performing potential energy variance minimization, the peak torque over the workspace comes out to be more than the unbalanced case.

$$A_{min} = [33.9\,\mathrm{N/rad}\ 0^{\circ}]^T$$

Potential energy variance minimization fails to provide balancing with torsional springs. Using this minima the peak torque obtained is 2.76 Nm, which is 12.65% higher than the peak torque obtained when the link is unbalanced, i.e., 2.45 Nm.

At this juncture a need was felt to look into a different method for balancing. Thus a new method was devised called peak torque minimization.

4.3 Peak Torque Minimization

4.3.1 Optimization Formulation

Peak torque minimization is also an optimization based technique. It is quite similar to the potential energy variance technique in the manner of implementation but the objective function here is taken as the peak torque of the mechanism over the entire workspace. A mesh is created over the configuration space and at every node of the mesh the torque required to keep the mechanism static at that point is calculated. This is done by using the relation, $\tau = \nabla PE$.

$$PE = f(\mathbf{x}, \mathbf{y}, K_1, K_2, ..., K_n). \tag{4.10}$$

To calculate torque for i^{th} actuator

$$\tau_i = \nabla PE = \frac{\partial PE}{\partial \theta_i} \tag{4.11}$$

For each set of $A = (\mathbf{y}, K_1, K_2, ..., K_n)$, the τ at every $\mathbf{x}$ in space is found. Let the set of all the τ for a particular A be τ_A.

$$\tau_{max} = max(\tau_A) \tag{4.12}$$

The optimization is set up as follows.

$$\begin{aligned} \text{Objective Function :} &\quad \tau_{max} \\ \text{Control Variable :} &\quad A \\ \text{Compulsory Constraint :} &\quad K_i \geq 0 \text{ for all } i = 1, ..., n \end{aligned} \tag{4.13}$$

4.3.2 Comparison of techniques

This optimization technique was compared with potential energy variance minimization. For doing so a new parameter called energy consumption (E) was introduced. E is defined as the energy consumed by an actuator to move the relevant links over the entire workspace in a specific pre-defined path. Defining a path that goes over the entire workspace is necessary because this is a non-conservative system. Energy consumed is path dependent.

$$E_i = \sum_{j=1}^{j=s} \left|\tau_i^j\right| \triangle\theta_i^j \tag{4.14}$$

where s is the number of grid points in the workspace.

The parameters used to compare the two optimization techniques were - Peak Torque and Energy as defined in equation 4.14.

See Table 4.2 and Figure 4.5 for comparison between peak torque and energy values for the two optimization methods studied for the case of balancing of a single link using coil springs.

Table 4.2: Potential energy variance minimization and peak torque minimization for a single link with non-zero-free length spring

Technique	Peak Torque	Energy	Minima
	τ_{max}(Nm)	E (Joules)	[K(N/m) len(m)]
PE Variance Minimization	0.26	0.78	[161.34 0.05]
Peak Torque Minimization	0.23	0.91	[167.26 0.05]

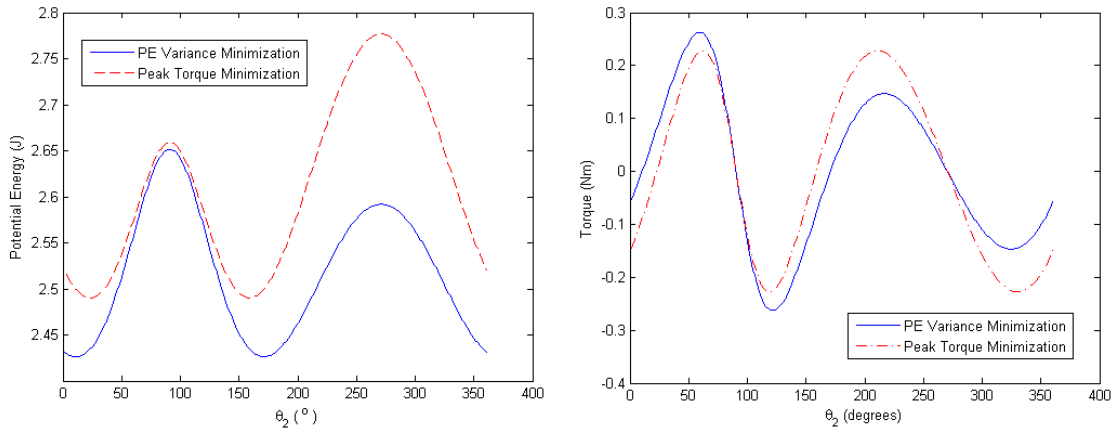

(a) (b)

Figure 4.5: Potential Energy (a) and Torque comparison (b) of the two techniques for a single link

Major differences between the results of the two optimizations -

1. Peak torque was slightly lower for the result of peak torque minimization compared to that for the potential energy variance minimization

2. Energy consumption for a run over the entire workspace was slightly higher for peak torque minimization as compared to potential energy variance minimization

Based on the design requirements for a certain mechanism, i.e., if a lower peak torque to use a lower end actuator is required or an overall reduction in energy consumption is sought after, one of these two optimization techniques can be used. If a combination of both is required then the objective function can be a linear combination of the normalized peak torque and normalized energy with appropriate weights.Let us use this technique and look into balancing with torsional springs again picking from where we left in section 4.2.

Using peak torque minimization the minima obtained is

$$A_{min} = [18.3\,\mathrm{N/rad}\ 38^{\circ}]^T \tag{4.15}$$

See table 4.3 for results. See figure 4.6 for torque variation with coil springs designed using peak torque minimization.

Table 4.3: Comparison of results for a single link before and after balancing using potential energy variance minimization

Case	Peak torque (Nm)	Energy (J)
Unbalanced	2.45	4.9
PE Variance Minimization	2.76	2.3
Peak Torque Minimization	1.48	2.7

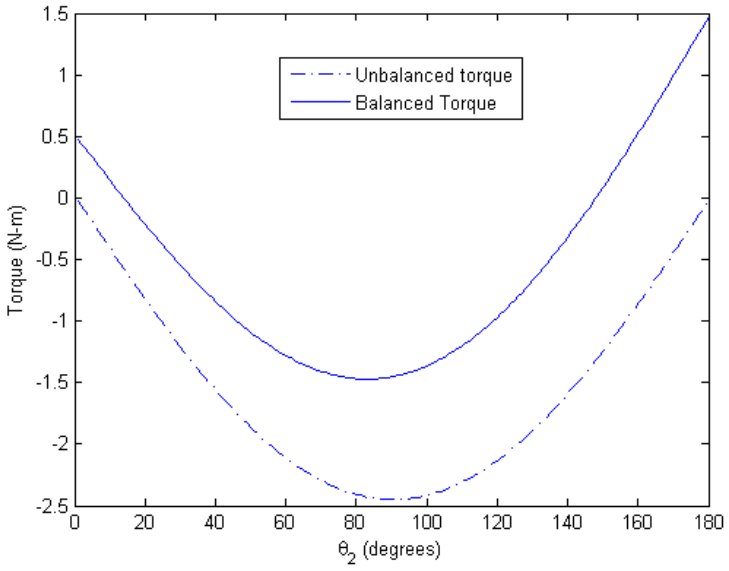

Figure 4.6: Plot of single link torsional spring balancing with peak torque minimization

This chapter applies approximate balancing of mechanisms using gas springs and

torsional springs. Peak torque minimization is proposed and compared with potential energy variance minimization. The two techniques give different results. The overall energy consumption is lower for potential energy variance minimization whereas the peak torque is lower for peak torque minimization. Upto this chapter we discussed how to design and locate springs for balancing different mechanisms, in the next chapter we will look into the effect of spring balancing on single-axis and polycentric lower-limb prosthesis.

CHAPTER 5

Spring Balancing of a Prosthesis

Spring balancing should be applicable on a prosthesis as well. It would be extremely efficacious if it could be implemented on a trans-femoral prosthesis because the users with trans-femoral prosthesis have to control a greater weight with a lower residual muscle strength. In this section we would be studying the effects of spring balancing on a polycentric knee trans-femoral prosthesis. The prosthetic knee used for the analysis is a commercially available four bar polycentric knee called Pendulum marketed by Ohio Willow Wood. The anthropometric data was borrowed from Winter (2009).

Human walking has two distinct phases - swing phase and stance phase. Figure 5.1 shows the different phases of human gait. In that figure the black leg is the one under consideration.

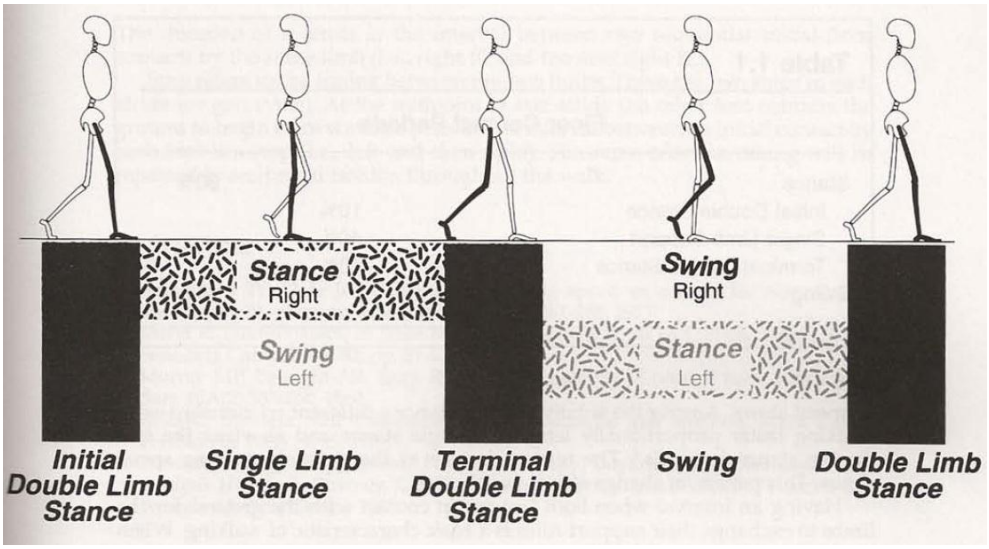

Figure 5.1: Phases of gait (Figure Courtesy Perry and Burnfield (1993))

Stance phase is that phase for a particular leg when it is in contact with the ground whereas swing phase is when the leg is in the air and moving forward for the next step.

So far in this work we have just looked into the torque of the leg in swing phase using the gradient of potential energy. For finding the hip moment in stance phase we will use the concepts laid down by Radcliffe (1994) in his work on prosthesis alignment.

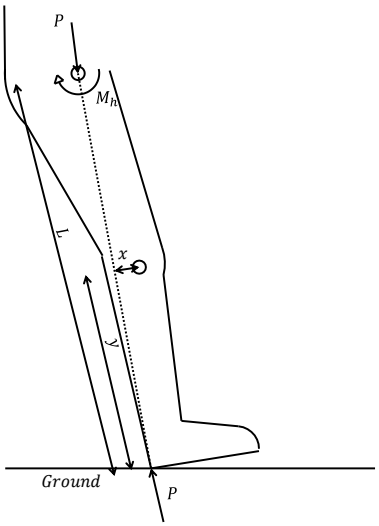

Figure 5.2: Stance phase hip moment

In figure 5.2,

- L is the distance between the point of contact of the foot on the ground and the hip joint along the line passing through those points(P-P).
- y is the distance between the knee joint and the point of contact on the ground along the line P-P.
- x is the perpendicular distance between the line P-P and the knee joint.

Radcliffe defines Hip moment as,

$$M_h = Pl\frac{x}{y} \tag{5.1}$$

Equation 5.1 is used to compute the hip moment during the stance phase of the leg. From that equation we can say that if y is more then M_h is lower. A polycentric fourbar prosthesis utilizes this concept. The instant centre of the fourbar is further up than the location of the anatomical knee. This increases the y, hence flexion becomes easy. The instant centre comes down so that it matches with the anatomical knee joint in the sitting position. Doing so is important for cosmetic purposes. Figure 5.3 shows the instant centre curve of the pendulum knee used in this analysis.

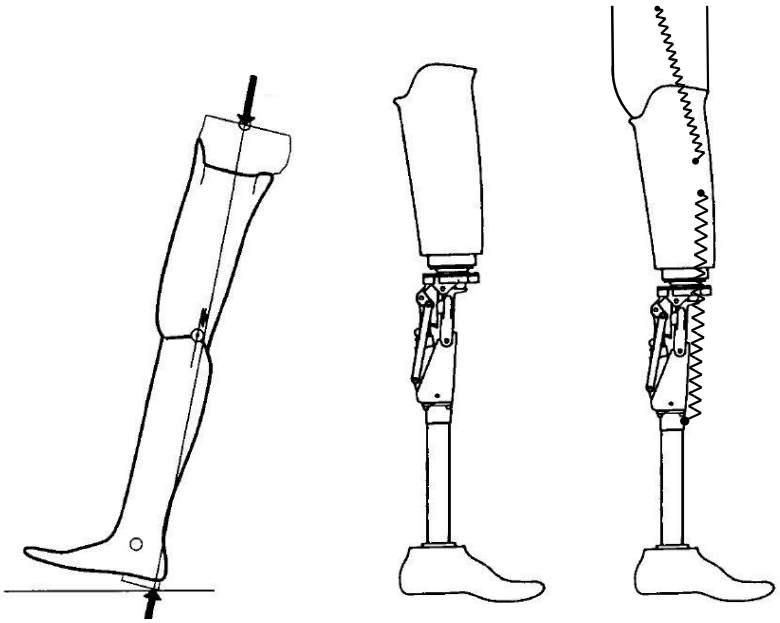

Figure 5.4: Schematic of Trans-femoral single pivot knee (left), four bar knee (centre) and spring balanced fourbar knee (right) prosthesis (Figure Courtesy Radcliffe (1994))

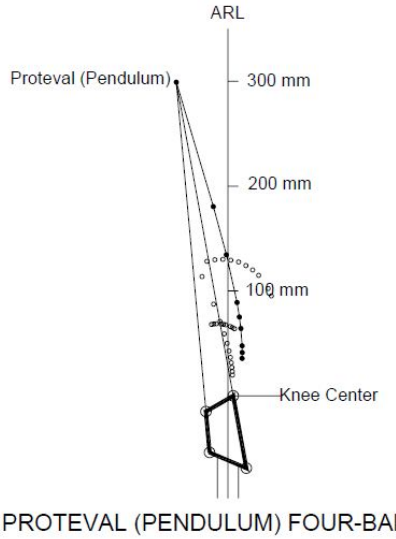

Figure 5.3: IC curve of pendulum knee(Figure Courtesy Radcliffe and Deg (2003))

Thus, using the relation from Radcliffe (1994) and gait data from Winter (2009), the hip moment was plotted for one complete gait cycle for a single axis trans-femoral prosthesis, polycentric (Pendulum knee) trans-femoral prosthesis and spring balanced polycentric (Pendulum knee) trans-femoral prosthesis. The schematic of all the three cases for which hip moment plots were generated are shown in figure 5.4.

Hip moment alone is considered in this analysis because the users of trans-femoral prosthesis can apply only hip moment. To verify the simulations figure 5.5 was compared with the experimental results published by Miller and Childress (2005). See figure 5.5 on the left for the simulations and on the right for the experimental results. In the experimental plot, the dotted line is for single axis while solid gray line is for polycentric.

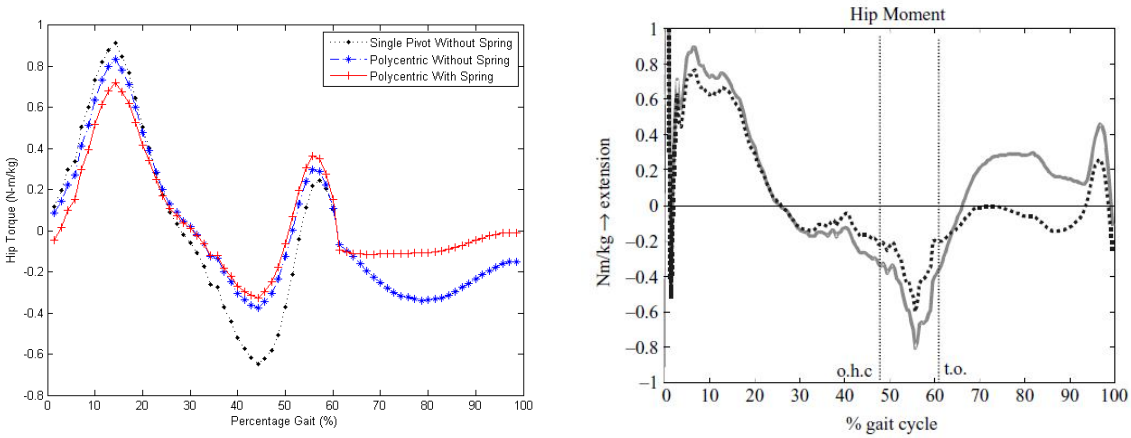

(a) (b)

Figure 5.5: Comparison of hip moment simulation (a) and experimental Hip Moment (b) (Figure adapted from Miller and Childress (2005))

The two plots in figure 5.5 match quite closely apart from the peak obtained in the simulation before the initiation of swing phase. This may be a result of the approximation that P as shown in figure 5.2 is the total ground reaction force acting on the foot. In reality there will be a component of the ground reaction force acting perpendicular to P, although in most phases of stance it is negligible compared to the magnitude of P. Moreover our analysis assumes the foot to be quasi-static at all positions whereas in the real experiment there would be inertial forces as well.

From figure 5.5 we can infer that using a spring reduces the hip moment required to walk with a prosthesis in both swing and stance phase although it is more effective in the swing phase. This is understandable because the springs were designed for balancing in the swing phase. The analysis carried out in this chapter confirms that spring balancing would be useful for lower limb prosthetic or orthotic devices in both swing and stance phase. In the next chapter we will design an experimental setup to physically realize spring balancing of human lower limb extremity in ambulation.

CHAPTER 6

Design of experimental setup

Preparation of an experimental setup for a person to wear a spring balanced lower limb orthosis for experimentally obtaining the hip and knee moment values while walking was looked into. A hip-knee-ankle polio brace was procured and alterations were made to that polio brace for developing a spring balanced lower limb orthosis in the same manner as shown in the figure 3.3.

An unanticipated challenge that was faced while designing was the reaction force of the hip joint spring shown in figure 6.1. The reaction force of the springs was extremely high. This force would be acting on the pelvis of the user. See figure 3.3 for the reaction force components acting on the pelvis by the hip joint spring. Such a high value of force acting periodically while walking could be very damaging for the body of the user.

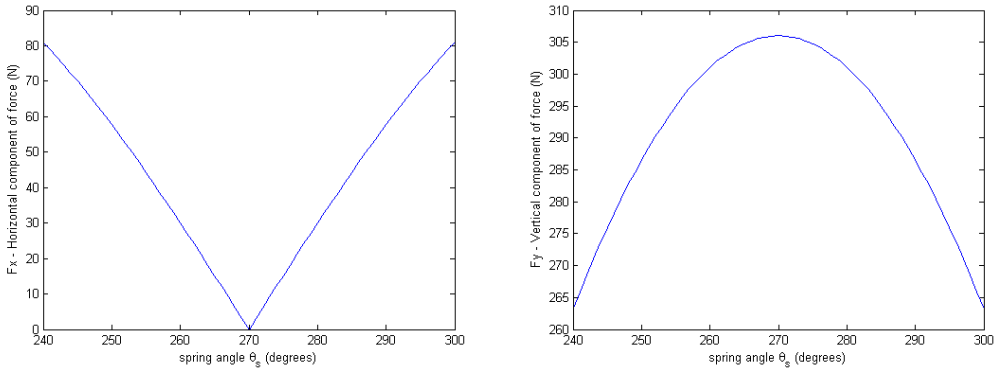

(a) (b)

Figure 6.1: Horizontal (a) and Vertical (b) components of the force on the pelvis

The vertical force would be taken care of by the orthosis itself. Horizontal force remains the main concern. This force could be distributed along the back of the user to eliminate localized effect of force. Before going for a mobile setup it was decided that a stationary setup would be designed where the person could wear the orthosis and walk on a treadmill. The hip-joint springs would be attached to a fixed frame and not to the trunk of the user. The frame would take care of the reaction forces.

The frame to be designed for this purpose had certain requirements -

- The frame should be modular and easy to transport

- The height and width of the orthosis should be adjustable based on the user
- The orthosis should be easily separable from the frame to allow different users to use the same frame

Since the frame had to be modular, a truss structure was found to be appropriate. A truss structure was designed such that the two contacts of the truss with the ground be pivots and there are no rollers.

The truss structure shown in figure 6.2 was designed.

Let n be the number of members in the truss and j be the number of pivots.

$$m = 3n - 2j \tag{6.1}$$

$$n = 6,\ j = 9 \tag{6.2}$$

$$m = 0 \tag{6.3}$$

Thus a statically determinate structure is obtained with the configuration shown in figure 6.2. The length of link 1 was chosen as 30 cm, link 3 as 54 cm and link 6 as 110 cm based on the anthropometric data on human height and the adjustability that is needed. Height adjustability was kept as 30 cm, hence the length of link 1 was chosen as that. The frame is designed to accommodate a user between 5 feet to 6 feet of height.

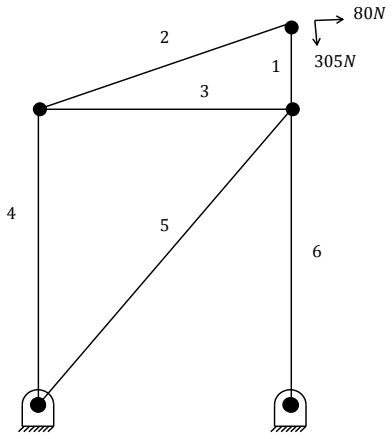

Figure 6.2: Schematic of the designed truss

The maximum horizontal and vertical force were applied to the top most point of the truss simultaneously. This is a conservative approach as the horizontal and vertical force are never maximum simultaneously. The force on all truss members was calculated using the method of joints with the convention that tension is positive while compression is negative. The following forces were found in the truss members,

$$
\begin{aligned}
T_1 &= -349.4\,\mathrm{N} \\
T_2 &= 91.5\,\mathrm{N} \\
T_3 &= -80\,\mathrm{N} \\
T_4 &= 44.4\,\mathrm{N} \\
T_5 &= 181.5\,\mathrm{N} \\
T_6 &= -512.4\,\mathrm{N}
\end{aligned}
$$

Stainless steel square cross sectioned hollow channels were chosen to be used as the material for truss members because they provide a good moment of inertia with lower weight and provide sufficient surface for fixing studs or bolts.

The major failure concern with the truss members is buckling of the compression members. The longest member has the greatest chance of buckling. Link 6 is the longest and has the highest compressive force as well.

Steel channel of outer square size 20 mm and material thickness 2 mm was available, hence calculations were done assuming those dimensions. See figure 6.3.

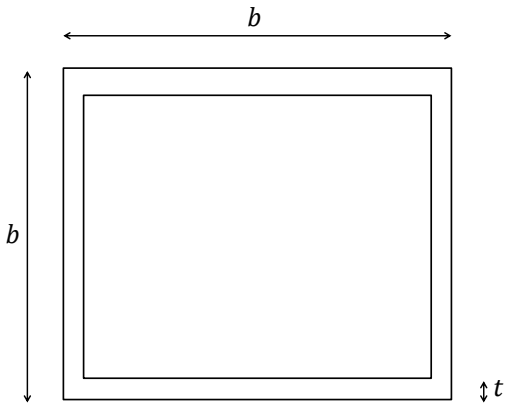

Figure 6.3: Illustration of the cross section of box channel

The moment of inertia for the box channel is given by equation 6.4

$$I = \frac{1}{6}bt^3 + \frac{1}{2}bt(b-t)^2 + \frac{1}{6}t(b-2t)^3. \tag{6.4}$$

Using b as 20 mm and t as 2 mm,

$$I = 7.872{\times}10^{-9}\, m^4$$

Critical buckling force for a rod pivoted at both ends is given by equation 6.5,

$$P_{cr} = \frac{\pi^2 E_{SS} I}{l^2}, \tag{6.5}$$

$$E_{SS} = 200\,\mathrm{GPa}.$$

The factor of safety obtained using equation 6.5 was,

$$FoS = 25 \tag{6.6}$$

25 seems like an over design but we would still continue with the same SS channel because they have to handle bending as well. As the load acting on the truss structure is not in the same plane as that of the truss, there would be some bending moment on the truss. The design approach should be kept conservative because if the design fails, it has the potential of hurting the user.

A single link of the truss is assumed to be taking all the bending alone as a cantilever beam.

$$M = 79.5\, Nm \tag{6.7}$$

$$y = 10\, mm \tag{6.8}$$

$$\sigma = \frac{My}{I} = 101\, MPa \tag{6.9}$$

$$\sigma_y = 250\,\mathrm{MPa} \tag{6.10}$$

$$FoS = 2.47 \tag{6.11}$$

The springs as designed in section 3.1 for the lower limb orthosis are tension springs.

They will have a hook at their end which would be slipped onto a metal rod as shown in figure 6.4. The design of that rod needs to be looked into. As the material of the shank of the orthosis is SS, these rods were also chosen to be made out of SS. The manufacturing procedure would require drilling a hole in the shank followed by an interference fit of the spring attachment rod. For greater rigidity, these rods can be welded once an interference fit has been made.

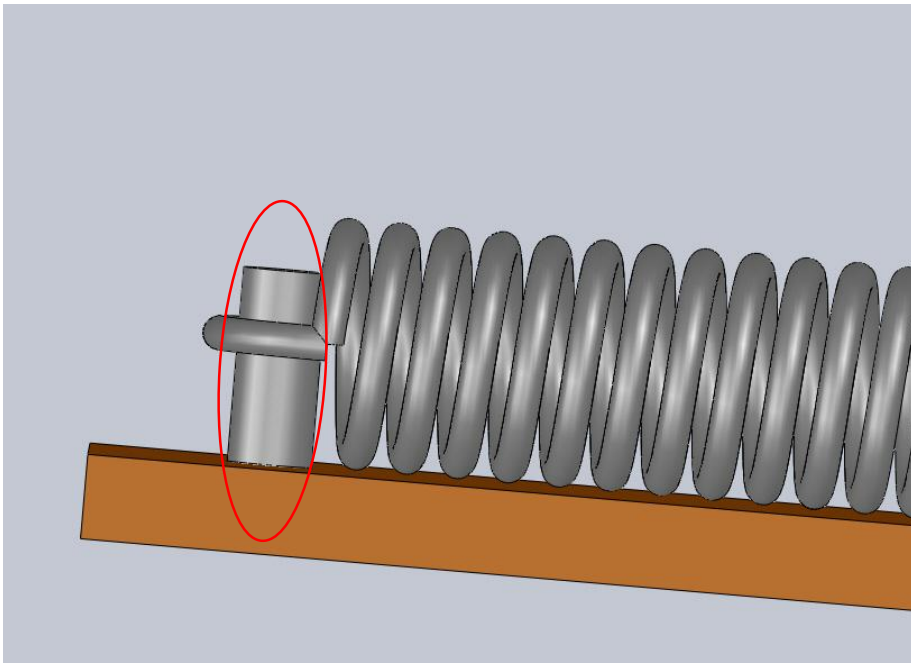

Figure 6.4: Spring attachment rod

$$r = 5\,mm \tag{6.12}$$

$$I = \frac{\pi r^4}{4} = 4.91 \times 10^{-10}\,m^4 \tag{6.13}$$

$$F_{max} = 305\,N \tag{6.14}$$

$$M_{max} = F_{max}(20\,mm) = 6.1\,Nm \tag{6.15}$$

$$\sigma = \frac{M_{max}y}{I} = 62.2\,MPa \tag{6.16}$$

$$FoS = \frac{\sigma_y}{\sigma} = 4 \tag{6.17}$$

A solid works model was prepared as shown in figure 6.5. The frame was designed

to fit a treadmill available at SpasTN, Chennai.

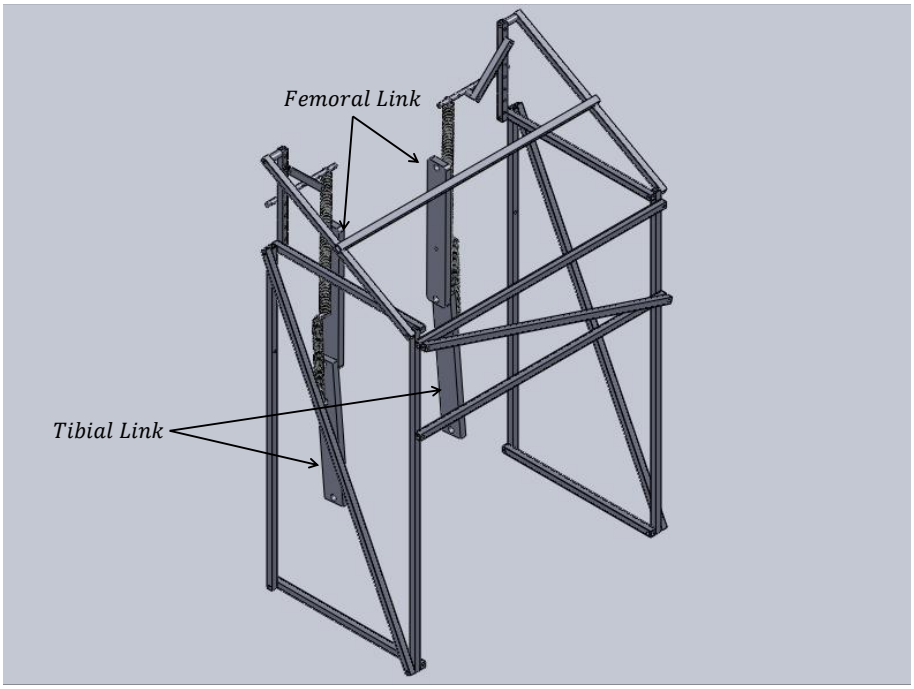

Figure 6.5: CAD model of the experimental setup

The frame can be adjusted for a users height and width. See figure 6.6. The link marked by red has multiple holes in it. The horizontal link can be fixed on any of these holes thus the height can be altered at intervals of 4 cm. Similarly the horizontal link marked with brown provides width adjustability. The diagonal link connecting the horizontal and vertical links with holes can be adjusted accordingly.

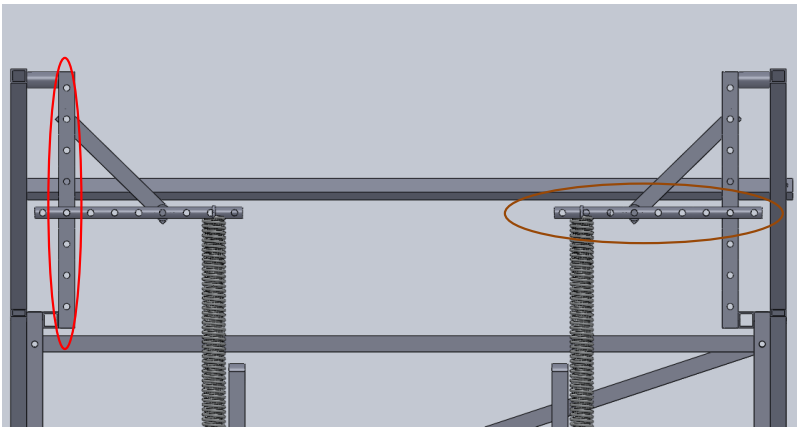

Figure 6.6: Frame adjustments

A finite element stress analysis of the frame was carried out with appropriate loads. See figure 6.7. The minimum factor of safety was found out to be 1.3.

Figure 6.7: Finite Element Simulation result

In this chapter we design a safe structure to take the load of spring balancing. The frame that takes the load was made adjustable to accommodate for users of different height and width. This frame with the lower-limb orthosis would serve as a test rig for experimentally verfiying the approximate spring balancing technique, potential energy variance minimization, which was the central theme of this work.

CHAPTER 7

Conclusion

This work resulted in the development of a new technique for spring balancing that borrows the methodology of constant potential energy and fuses it with numerical optimization yielding a method that provides immense flexibility and practical application.

This method is used for simulation of spring balancing under various scenarios - open chain planar linkages, closed chain planar linkages, open chain spatial linkages, balancing with gas spring and balancing with torsional spring. Spring balancing of a lower limb orthosis was investigated in detail and a stationary setup was designed. The manufacturing of the setup is yet to start. The effect of spring balancing on a transfemoral prosthesis user was also investigated.

Overall this work paves the way towards development of an active exoskeleton and passive prosthetic & orthotic devices which people with weak muscular strength may be able to control with their residual strength.

Future work would involve - Integration of singular-solution-elimination in the proposed spring balancing technique itself ; Modification of the technique to suit the application of prosthetic limbs could also be looked into ; Design of a mobile spring-balanced-lower-limb-orthosis unit ; Experimental verification of the results obtained in this work.

REFERENCES

1. **Agrawal, A.** and **S. K. Agrawal** (2005). Design of gravity balancing leg orthosis using non-zero free length springs. *Mechanism and Machine Theory*, **40**(6), 693–709.

2. **Agrawal, S. K.**, **S. K. Banala**, **A. Fattah**, **V. Sangwan**, **V. Krishnamoorthy**, **J. R. Scholz**, and **W. L. Hsu** (2007). Assessment of motion of a swing leg and gait rehabilitation with a gravity balancing exoskeleton. *IEEE Transactions On Neural Systems and Rehabilitation Engineering*, **15**(3), 410–420.

3. **Agrawal, S. K.** and **A. Fattah** (2004*a*). Gravity-balancing of spatial robotic manipulators. *Mechanism and Machine Theory*, **39**(12), 1331–1344.

4. **Agrawal, S. K.** and **A. Fattah** (2004*b*). Theory and design of an orthotic device for full or partial gravity-balancing of a human leg during motion. *IEEE Transactions On Neural Systems and Rehabilitation Engineering*, **12**(2), 157–165.

5. **Banala, S. K.**, **S. K. Agrawal**, **A. Fattah**, **V. Krishnamoorthy**, **W. L. Hsu**, **J. Scholz**, and **K. Rudolph** (2006). Gravity-balancing leg orthosis and its performance evaluation. *IEEE Transactions On Robotics*, **22**(6), 1228–1239.

6. **Brinkman, M. L.** and **J. L. Herder** (2002). Optimizing a balanced spring mechanism. *Proceedings of the ASME DETC, Montreal, Canada, September*.

7. **Chaudhari, H.** (2012). Design of a standing wheelchair. Dual degree project report, IIT Madras.

8. **Ciupitu, L.** and **I. Simionescu** (). Static balancing of mechanical systems used in medical engineering field–approximate balancing. *Romanian Journal of Technical Science*, 19–20.

9. **Deepak, S.** and **G. Ananthasuresh** (2012). Perfect static balance of linkages by addition of springs but not auxiliary bodies. *Journal of Mechanisms and Robotics*, **4**(2).

10. **Deepak, S. R.** and **G. Ananthasuresh**, Static balancing of spring-loaded planar revolute-joint linkages without auxiliary links. *In 14th National Conference on Machines and Mechanisms, Dec*. 2009.

11. **Fattah, A.**, **S. K. Agrawal**, **G. Catlin**, and **J. Hammnett** (2006). Design of a passive gravity-balanced assistive device for sit-to-stand tasks. *Journal of Mechanical Design*, **128**(5), 1122–1129.

12. **Gopalswamy, A.**, **P. Gupta**, and **M. Vidyasagar**, A new parallelogram linkage configuration for gravity compensation using torsional springs. *In Robotics and Automation, 1992. Proceedings., 1992 IEEE International Conference on*. IEEE, 1992.

13. **Grace, A.** and **M. Works**, *Optimization Toolbox: For Use with MATLAB: User's Guide*. Math works, 1990.

14. **Huang, C.** and **B. Roth** (1993). Dimensional synthesis of closed-loop linkages to match force and position specifications. *Journal of Mechanical Design*, **115**, 194.

15. **Huang, C.** and **B. Roth** (1994). Position-force synthesis of closed-loop linkages. *Journal of Mechanical Design*, **116**, 155.

16. **Lesjoforbs** (2013). Spring characteristics. http://www.lesjoforsab.com/gas-springs/spring-characteristics.asp.

17. **Mahalingam, S.** and **A. Sharan**, The optimal balancing of the robotic manipulators. *In Robotics and Automation. Proceedings. 1986 IEEE International Conference on*, volume 3. IEEE, 1986.

18. **Miller, L. A.** and **D. S. Childress** (2005). Problems associated with the use of inverse dynamics in prosthetic applications: an example using a polycentric prosthetic knee. *Robotica*, **23**(03), 329–335.

19. **Nakayama, T.**, **Y. Araki**, and **H. Fujimoto**, A new gravity compensation mechanism for lower limb rehabilitation. *In Mechatronics and Automation, 2009. ICMA 2009. International Conference on*. IEEE, 2009.

20. **Norton, R.**, *Machine design: an integrated approach*. Prentice-Hall New York, 1996.

21. **Perry, J.** and **J. M. Burnfield**, *Gait analysis: normal and pathological function*. Slack, 1993.

22. **Radcliffe, C.** (1994). Four-bar linkage prosthetic knee mechanisms: kinematics, alignment and prescription criteria. *Prosthetics and orthotics international*, **18**(3), 159–173.

23. **Radcliffe, C. W.** and **M. Deg** (2003). Biomechanics of knee stability control with four-bar prosthetic knees. *ISPO, Prosthetic and Orthotics International, Melbourne*.

24. **Rahman, T.**, **R. Ramanathan**, **R. Seliktar**, and **W. Harwin** (1995). A simple technique to passively gravity-balance articulated mechanisms. *Transaction-American Society of Mechanical Engineers Journal of Mechanical Design*, **117**, 655–657.

25. **Rahman, T.**, **W. Sample**, **R. Seliktar**, **M. Alexander**, **M. Scavina**, *et al.* (2000). A body-powered functional upper limb orthosis. *Journal of rehabilitation research and development*, **37**(6), 675–680.

26. **Segla, S.**, **C. Kalker-Kalkman**, and **A. Schwab** (1998). Statical balancing of a robot mechanism with the aid of a genetic algorithm. *Mechanism and Machine Theory*, **33**(1), 163 – 174. ISSN 0094-114X.

27. **Streit, D.** and **E. Shin** (1993). Equilibrators for planar linkages. *Journal of mechanical design*, **115**(3), 604–611.

28. **SuperGasSprings** (2007). Compression gas spring technical specifications. URL `http://www.gasprings.com/comgas.htm`.

29. **Te Riele, F. L.** and **J. L. Herder**, Perfect static balance with normal springs. *In Proceedings of the ASME Design Engineering Technical Conferences, Pittsburg, Pennsylvania*. 2001.

30. **Titaneps** (2012). Gas spring schematic. URL `http://www.titaneps.com/gas-springs`.

31. **Winter, D. A.**, *Biomechanics and motor control of human movement*. John Wiley & Sons, 2009.